ESAIM: M2AN 50 (2016) 783–808
DOI: 10.1051/m2an/2015066

**ESAIM: Mathematical Modelling and Numerical Analysis**
www.esaim-m2an.org

# A PLANE WAVE VIRTUAL ELEMENT METHOD FOR THE HELMHOLTZ PROBLEM

Ilaria Perugia[1,2], Paola Pietra[3] and Alessandro Russo[4]

**Abstract.** We introduce and analyze a virtual element method (VEM) for the Helmholtz problem with approximating spaces made of products of low order VEM functions and plane waves. We restrict ourselves to the 2D Helmholtz equation with impedance boundary conditions on the whole domain boundary. The main ingredients of the plane wave VEM scheme are: (i) a low order VEM space whose basis functions, which are associated to the mesh vertices, are not explicitly computed in the element interiors; (ii) a proper local projection operator onto the plane wave space; (iii) an approximate stabilization term. A convergence result for the $h$-version of the method is proved, and numerical results testing its performance on general polygonal meshes are presented.

**Mathematics Subject Classification.** 65N30, 65N12, 65N15, 35J05.

Received April 14, 2015. Revised August 11, 2015.
Published online May 23, 2016.

## 1. Introduction

The Virtual Element Method (in short, VEM) is a generalization of the classical finite element method recently introduced in [5,10]. The key features of the VEM are:

- the decomposition of the computational domain can consist of arbitrary polygons in 2D and polyhedra in 3D;
- the local spaces, in general, contain polynomials, as in the classical finite elements, but include also more general functions (usually defined through a differential operator) whose pointwise values need not to be computed (hence the name "Virtual");
- the VEM passes the Patch Test.

The basic VEM introduced on the Poisson problem has then been extended to highly regular [4], non conforming [2] and discontinuous approximating spaces [15], to general elliptic [9] and mixed problems [7,8,16], as well as to Stokes [1], plate problems [14], linear and non linear elasticity [6,11,26], and fluid flows in fractured media [12].

*Keywords and phrases.* Helmholtz equation, virtual element method, plane wave basis functions, error analysis, duality estimates.

[1] Faculty of Mathematics, University of Vienna, 1090 Vienna, Austria. ilaria.perugia@univie.ac.at

[2] Department of Mathematics, University of Pavia, 27100 Pavia, Italy.

[3] Istituto di Matematica Applicata e Tecnologie Informatiche "Enrico Magenes", CNR, 27100 Pavia, Italy. paola.pietra@imati.cnr.it

[4] University of Milano Bicocca, 20126 Milano, Italy. alessandro.russo@unimib.it

In this paper, we aim at extending the VEM approach to an indefinite problem. More precisely, we present and analyze a new method, based on inserting plane wave basis functions within the VEM framework, in order to construct a conforming, high order method for the discretization of the Helmholtz equation. As in the partition of unity method (PUM, see *e.g.*, [38–40]), we use approximation spaces made of products of functions that constitute a partition of unity and plane waves.

Plane wave functions are a particular case of Trefftz functions for the Helmholtz problem, *i.e.*, functions belonging to the kernel of the Helmholtz operator. Other Helmholtz–Trefftz functions are, *e.g.*, circular/spherical waves (also denoted as Fourier-Bessel functions, or generalized harmonic polynomials), or Hankel functions. The idea of inserting Trefftz basis functions within the approximating spaces in finite element discretizations of the Helmholtz problem is motivated because these spaces possess better approximation properties for Helmholtz solutions, compared to standard polynomial spaces (see, *e.g.*, [43]), thus similar accuracy can be obtained with less degrees of freedom. This mitigates the strong requirements in terms of number of degrees of freedom per wavelength due to the pollution effects [3].

There are in the literature several finite element methods for the Helmholtz problem which make use of Trefftz functions. Besides the already mentioned PUM, which is $H^1$-conforming, other approaches use discontinuous Trefftz basis functions and impose interelement continuity with different strategies: by least square formulations (see [44, 47]); within a discontinuous Galerkin (DG) framework (like the ultra weak variational formulation (UWVF) [18,19] or its Trefftz-DG generalization [28,30,31]; see also [17,24] for the derivation of the UWVF as a Trefftz-DG method); by the use of Lagrange multipliers (see, *e.g.*, [22,23,34,49]); through weighted residual formulations (like in the variational theory of complex rays [36,46], or in the wave based method [20,21]). We refer to the recent survey [32] for details.

As a first construction of a plane wave-virtual element method (PW-VEM), we focus here on the 2D Helmholtz problem with impedance boundary conditions on the whole domain boundary. We restrict ourselves to low order VEM functions and we take a uniform plane wave enrichment of the approximating spaces. On polygonal meshes, our basis functions will be then products of low order VEM functions associated to the mesh vertices, multiplied by a linear combination of $p$ plane waves centered at the corresponding vertices.

In the VEM framework the basis functions are not explicitly computed in the elements interiors. A crucial step is the definition of a proper local projection operator onto a space that has to verify two major requirements: providing good approximation properties for the solution of the homogeneous Helmholtz problem, and allowing to compute exactly the bilinear form whenever one of the two entries belongs to that space (*consistency requirement*). For this reason, we define the local projector through the Helmholtz bilinear form onto the space of discontinuous plane wave functions.

The discrete bilinear form is then split into two parts: one that can be computed exactly, thanks to the projection operator, and a second one, that can be approximated, with the role of a stabilization term.

The analysis of the $h$-version of the method is given in an abstract form and a sufficient condition on the stabilization term that implies the discrete Gårding inequality (which in turn implies convergence) is provided. The continuity of the local projectors requires a minimal resolution condition for the mesh width $h$ (see Props. 2.1 and 2.3). This condition also emerges in the convergence analysis. There, quasi-optimality is proved under the standard threshold condition that $hk^2$ is sufficiently small (see Thm. 3.1 and Rem. 3.2).

The outline of the paper is as follows. We introduce the model problem and its PW-VEM discretization in Section 2, describing the approximating spaces and the projection operator, as well as all the relevant matrix blocks needed for the implementation; the choice of the stabilization operator is not specified at this stage. In Section 3, we prove an abstract convergence result of the $h$-version of the PW-VEM which, together with best approximation estimates for the considered approximating spaces, give convergence rates of the method, provided that continuity and Gårding inequality are satisfied for the discrete operator. A sufficient condition on the stabilization term that guarantees a Gårding inequality for the discrete operator is given in Section 4. An explicit form of a possible stabilization term is then provided. Finally, we numerically test in Section 5 the performance of the resulting PW-VEM.

## 2. The PW-VEM method

We introduce the PW-VEM method for the Helmholtz's problem. For simplicity, we consider the two-dimensional case.

Let $\Omega \subset \mathbb{R}^2$ be a bounded, convex polygon. Consider the Helmholtz boundary value problem

$$\begin{aligned} -\Delta u - k^2 u &= 0 \qquad \text{in } \Omega, \\ \nabla u \cdot \boldsymbol{\nu} + ik\, u &= g \quad \text{on } \partial\Omega, \end{aligned} \tag{2.1}$$

where the unknown $u$ is a complex-valued function, $k > 0$ is a given wave number (the corresponding wavelength is $\lambda = 2\pi/k$), $\boldsymbol{\nu}$ is the outer normal unit vector to $\partial\Omega$, and $i$ is the imaginary unit. To simplify the presentation, we are considering impedance boundary conditions on the whole $\partial\Omega$, with datum $g \in L^2(\partial\Omega)$.

Since we are interested in the mid- and high-frequency regimes, we assume that $\lambda < \operatorname{diam}(\Omega)$ or, equivalently, $k > 2\pi/\operatorname{diam}(\Omega)$.

The variational formulation of (2.1) reads as follows: find $u \in H^1(\Omega)$ such that

$$b(u,v) = a(u,v) + ik \int_{\partial\Omega} u\overline{v}\,\mathrm{d}S = \int_{\partial\Omega} g\overline{v}\,\mathrm{d}S \qquad \forall v \in H^1(\Omega), \tag{2.2}$$

where

$$a(u,v) = \int_\Omega \nabla u \cdot \overline{\nabla v}\,\mathrm{d}V - k^2 \int_\Omega u\overline{v}\,\mathrm{d}V;$$

see, *e.g.* Proposition 8.1.3 of [38] for the well-posedness of the variational problem (2.2).

### 2.1. Discretization spaces

Let $\mathcal{T}_h = \{K\}$ be a mesh of the domain $\Omega$ made of polygons $K$ with mesh width $h$, *i.e.*, $h = \max_{K\in\mathcal{T}_h} h_K$, where $h_K$ is the diameter of $K$. Given $K \in \mathcal{T}_h$, we denote by $\mathbf{x}_K$ the mass center of $K$, and by $\boldsymbol{\nu}_K$ the unit normal vector to $\partial K$ pointing outside $K$. Moreover, we denote by $n_K$ the number of edges $e$ of K, and by $V_j$ and $\mathbf{x}_j$, $j = 1,\dots,n_K$, the vertices of $K$ and their coordinates, respectively.

Let $K$ be an element of $\mathcal{T}_h$. First of all we choose the VEM space as the (local) finite dimensional space $V(K)$ defined as

$$V(K) = \{v \in H^1(K), v_{|\partial K} \in C^0(\partial K),\ v_{|e} \in \mathbb{P}_1(e)\ \forall e \subset \partial K, \Delta v = 0 \text{ in } K\}. \tag{2.3}$$

Here and in the following, we denote by $\mathbb{P}_1(D)$ the space of polynomials of degree at most one in the domain $D$. The functions in $V(K)$ are completely determined by their value in the $n_K$ vertices. The dimension of $V(K)$ is equal to $n_K$. We denote by $\{\varphi_j\}_{j=1}^{n_K}$ the canonical basis functions in $V(K)$ defined by

$$\varphi_j(V_i) = \delta_{ij}, \quad i,j = 1,\dots,n_K.$$

Notice that $\mathbb{P}_1(K) \subseteq V(K)$, and $\mathbb{P}_1(K) = V(K)$ if and only if $n_K = 3$, *i.e.*, $K$ is a triangle.

The basis $\{\varphi_j\}_{j=1}^{n_K}$ is a partition of unity, *i.e.*, $f(\mathbf{x}) = \sum_{j=1}^{n_K} \varphi_j(\mathbf{x}) = 1$ for all $\mathbf{x} \in K$. In fact, since the functions $\varphi_j$ are harmonic in $K$, linear on each $e \subset \partial K$, with $\varphi_j(V_i) = \delta_{ij}$, then $\Delta f = 0$ in $K$ and $f = 1$ on $\partial K$, which imply $f = 1$ in $K$.

Next, we introduce $p_K$ different normalized directions $\{\mathbf{d}_\ell\}_{\ell=1}^{p_K}$, and we define the local PW-VEM space

$$V_{p_K}(K) = \left\{ v :\ v = \sum_{j=1}^{n_K} \sum_{\ell=1}^{p_K} a_{j\ell}\, \varphi_j(\mathbf{x}) \mathrm{e}^{ik\mathbf{d}_\ell\cdot(\mathbf{x}-\mathbf{x}_j)},\ a_{j\ell} \in \mathbb{C} \right\}.$$

We also introduce the standard plane wave space (centered at $\mathbf{x}_K$)

$$V^*_{p_K}(K) = \left\{ v :\ v = \sum_{\ell=1}^{p_K} a_\ell\, \mathrm{e}^{ik\mathbf{d}_\ell\cdot(\mathbf{x}-\mathbf{x}_K)},\ a_\ell \in \mathbb{C} \right\}.$$

Clearly, $V^*_{p_K}(K) \subset V_{p_K}(K)$.

Setting, for $\ell = 1, \dots, p_K$ and $j = 1, \dots, n_K$,

$$\pi_\ell(\mathbf{x}) = \mathrm{e}^{ik\mathbf{d}_\ell\cdot(\mathbf{x}-\mathbf{x}_K)}, \quad \pi_{j\ell}(\mathbf{x}) = \mathrm{e}^{ik\mathbf{d}_\ell\cdot(\mathbf{x}-\mathbf{x}_j)},$$
$$\psi_r(\mathbf{x}) = \varphi_j(\mathbf{x})\,\pi_{j\ell}(\mathbf{x}), \qquad \text{with } r = (j-1)p_K + \ell,$$

we have

$$V_{p_K}(K) = \mathrm{span}\{\psi_r(\mathbf{x}),\ r = 1, \dots, n_K p_K\}.$$

Notice that $\pi_{j\ell}(\mathbf{x}) = c_{j\ell}\,\pi_\ell(\mathbf{x})$, where $c_{j\ell} = \mathrm{e}^{ik\mathbf{d}_\ell\cdot(\mathbf{x}_K-\mathbf{x}_j)}$.

Finally, in order to impose continuity across interelement boundaries, we choose $p_K = p$ and the same directions $\{\mathbf{d}_\ell\}_{\ell=1}^p$ for all $K \in \mathcal{T}_h$, and we define the global PW-VEM space as

$$V_p(\mathcal{T}_h) = \left\{v \in C^0(\overline{\Omega}) :\ v|_K \in V_p(K)\ \forall K \in \mathcal{T}_h\right\}.$$

The Galerkin approximation of problem (2.2) in the spaces $V_p(\mathcal{T}_h)$ gives rise to the PUM [38–40]. In this case, an explicit expression of the discrete functions $\psi_r$, and thus of the functions $\varphi_j$, is needed also in the element interiors. Since the functions of $V(K)$ are not explicitly known (unless $K$ is a triangle), one should change the definition of the space $V(K)$; possible choices can be found, *e.g.*, in [37, 48]. Moreover, the implementation of PUM requires the use of numerical quadrature on polygons. On the contrary, in the PW-VEM method we are going to define, by adopting the VEM framework, we do not need any explicit expression of the partition of unity functions $\varphi_j$, nor numerical quadrature on polygons.

We make the following assumptions on the meshes and on the plane wave directions:

(i) the elements $K \in \mathcal{T}_h$ are convex and with *non degenerating* sides, *i.e.*, there exists $C_{\mathrm{reg}} > 0$ independent of $h_K$ such that $\mathrm{length}(e) \le C_{\mathrm{reg}} h_K$ for every $e$ edge of $K$;

(ii) there exists an integer $m \ge 1$ such that
$$p = 2m + 1;$$

(iii) the directions $\{\mathbf{d}_\ell\}_{\ell=1}^p$ satisfy a minimum angle condition, *i.e.*, there exists $0 < \delta \le 1$ such that the minimum angle between two different directions is $\ge \frac{2\pi}{p}\delta$, and are such that the angle between two subsequent directions is $< \pi$.

Assumption (i) guarantees that the partition of unity $\{\varphi_j\}_{j=1}^{n_K}$ satisfies the assumptions of Theorem 2.1 from [39] used in the proofs of Theorem 3.1 and Proposition 3.3 below. Moreover, assumptions (i)–(iii) guarantee validity of approximation estimates in plane wave spaces (see [42, 43] and the proof of Prop. 2.1 below). The possibility of dealing with non convex elements, by modifying the definition of the VEM space, is discussed in Remark 3.5 below.

## 2.2. The projector $\Pi$

In the VEM framework, a crucial step is the choice of a local projection operator that allows to compute bilinear forms without resorting to the explicit form of the basis functions (the functions $\psi_r$ here). The space onto which we project has to fulfill two major requirements: providing good approximation properties for the solution of the problem at hand, and allowing to compute exactly the bilinear form whenever one of the two entries belongs to that space.

Here, we choose as space where projecting onto the space of (discontinuous) piecewise plane waves, which we denote by $V_p^*(\mathcal{T}_h)$, *i.e.*,

$$V_p^*(\mathcal{T}_h) = \prod_{K\in\mathcal{T}_h} V_p^*(K).$$

For any $K \in \mathcal{T}_h$, we define the local bilinear form

$$a^K(u, v) = \int_K \nabla u \cdot \overline{\nabla v}\,\mathrm{d}V - k^2 \int_K u\overline{v}\,\mathrm{d}V,$$

which is a local version of the bilinear form defining the variational problem (2.2), ignoring the boundary term.

We define the projector $\Pi : V_p(K) \to V_p^*(K)$ as follows:

$$a^K(\Pi u, w) = a^K(u, w) \qquad \forall w \in V_p^*(K). \tag{2.4}$$

The projector $\Pi$ is well-defined, provided that $k^2$ is not a Neumann–Laplace eigenvalue on $K$. This is guaranteed, for instance, when condition (2.5) below is satisfied (see Sect. 2.3 for more details).

Clearly, if $u \in V_p^*(K)$, then $\Pi u = u$. We observe that the right-hand side of (2.4) is independent of the values of the functions of $V(K)$ in the interior of $K$. In fact, for any $u \in V_p(K)$ and $w \in V_p^*(K)$, integrating by parts, we have

$$a^K(u, w) = \int_K \nabla u \cdot \overline{\nabla w}\, \mathrm{d}V - k^2 \int_K u\overline{w}\, \mathrm{d}V = \int_{\partial K} u\overline{\nabla w \cdot \boldsymbol{\nu}_K}\, \mathrm{d}S,$$

since $\Delta w + k^2 w = 0$. Therefore, in order to compute the right-hand side of (2.4) (and thus $\Pi$), we only need $u$ and $\nabla w \cdot \boldsymbol{\nu}_K$ on $\partial K$.

## 2.3. Continuity of the operator $\Pi$

Let $\mu_2$ be the smallest strictly positive eigenvalue of the Neumann–Laplace operator on $K$. In view of possible extensions to non convex elements, we consider here together the case of $K$ convex, for which $\mu_2 \geq \pi^2/h_K^2$ [45], and the case of $K$ star-shaped with respect to a ball, for which $\mu_2 \geq C_0\,\pi^2/h_K^2$, with $0 < C_0 \leq 1$ only depending on the shape of $K$ [13,35]. Therefore, assuming that

$$0 < h_K k \leq C_1 < \sqrt{C_0}\,\pi, \tag{2.5}$$

we guarantee that $k^2 < \mu_2$.

We denote by $\|\cdot\|_{0,D}$ the $L^2$-norm in the domain $D$, and define the weighted norm

$$\|v\|_{1,k,K}^2 = \|\nabla v\|_{0,K}^2 + k^2\,\|v\|_{0,K}^2 \qquad \forall v \in H^1(K).$$

The following discrete inf-sup condition holds true.

**Proposition 2.1.** *Provided that $h_K k$ satisfies*

$$h_K k \leq \alpha_0 < \min\left\{\frac{\sqrt{C_0}\,\pi}{\sqrt{2}}, 0.5538\right\}, \tag{2.6}$$

*($h_K k \leq \alpha_0 < 0.5538$ whenever $K$ is convex) there exists a positive constant $\beta = \beta(h_K k)$ (i.e., $\beta$ depends on $h_K$ and $k$ through their product $h_K k$), which remains uniformly bounded away from zero as $h_K k \to 0$, such that*

$$\forall v \in V_p^*(K) \quad \exists w \in V_p^*(K) \quad s.t. \quad \frac{a^K(v, w)}{\|w\|_{1,k,K}} \geq \beta(h_K k)\,\|v\|_{1,k,K}\,. \tag{2.7}$$

*Proof.* Assume, with no loss of generality, that the direction $\mathbf{d}_1^* = (1, 0)$ belongs to the set of directions $\{\mathbf{d}_\ell\}_{\ell=1}^p$. Due to our assumptions on the directions (see assumption (iii) at the end of Sect. 2.1), there are two directions $\mathbf{d}_2^*, \mathbf{d}_3^* \in \{\mathbf{d}_\ell\}_{\ell=1}^p$ such that $\mathbf{d}_1^*, \mathbf{d}_2^*, \mathbf{d}_3^*$ are listed in counterclockwise order, and the angles $\delta_1$, $\delta_2$, $\delta_3$ between $\mathbf{d}_3^*$ and $\mathbf{d}_1^*$, $\mathbf{d}_1^*$, and $\mathbf{d}_2^*$, $\mathbf{d}_2^*$ and $\mathbf{d}_3^*$, respectively, satisfy $0 < \sin\delta_1, \sin\delta_2, \sin\delta_3 \leq 1$.

Let $b_1 \in V_p^*(K)$ be defined as

$$b_1(\mathbf{x}) = \sum_{\ell=1}^{3} \alpha_\ell \mathrm{e}^{ik\mathbf{d}_\ell^* \cdot (\mathbf{x} - \mathbf{x}_K)},$$

with

$$\alpha_1 = \frac{\sin\delta_3}{\sin\delta_1 + \sin\delta_2 + \sin\delta_3}, \quad \alpha_2 = \frac{\sin\delta_1}{\sin\delta_1 + \sin\delta_2 + \sin\delta_3}, \quad \alpha_3 = \frac{\sin\delta_2}{\sin\delta_1 + \sin\delta_2 + \sin\delta_3}.$$

Since $\sum_{\ell=1}^3 \alpha_\ell = 1$, then $b_1(\mathbf{x}_K) = 1$. Moreover, since $\mathbf{d}_1^* = (1,0)$, $\mathbf{d}_2^* = (\cos\delta_2, \sin\delta_2)$ and $\mathbf{d}_3^* = (\cos\delta_1, -\sin\delta_1)$, we have $\sum_{\ell=1}^3 \alpha_\ell \mathbf{d}_\ell^* = \mathbf{0}$, and therefore $\nabla b_1(\mathbf{x}_K) = \mathbf{0}$.

The following bounds hold true:

$$\|b_1\|_{0,K} \le |K|^{1/2}, \tag{2.8}$$

$$\|1 - b_1\|_{0,K} \le \frac{1}{2}(h_K k)^2 |K|^{1/2}, \tag{2.9}$$

$$\|\nabla b_1\|_{0,K} \le h_K k^2 |K|^{1/2}. \tag{2.10}$$

The bound (2.8) follows from $\alpha_1, \alpha_2, \alpha_3 > 0$ and $\sum_{\ell=1}^3 \alpha_\ell = 1$:

$$\|b_1\|_{0,K}^2 = \int_K |b_1(\mathbf{x})|^2 \,\mathrm{d}V \le \int_K \Big(\sum_{\ell=1}^3 \alpha_\ell\Big)^2 \mathrm{d}V = |K|.$$

The bounds (2.9) and (2.10) immediately follow from Taylor's expansions of $b_1(\mathbf{x})$ and $\nabla b_1(\mathbf{x})$, taking into account that $b_1(\mathbf{x}_K) = 1$ and $\nabla b_1(\mathbf{x}_K) = 0$.

Fix $0 \neq v \in V_p^*$ and define $w$ as the unique element of $V_p^*$ such that

$$\int_K \nabla w \cdot \overline{\nabla \xi} \,\mathrm{d}V + k^2 \int_K w\, \overline{\xi} \,\mathrm{d}V = a^K(v,\xi) \qquad \forall \xi \in V_p^*. \tag{2.11}$$

Since the threshold condition (2.5) implies that $k^2 < \mu_2$, the right-hand side is a nonzero functional of $\xi$, therefore $w \neq 0$. Notice that, taking $\xi = v - w$ in (2.11), we have $\|\nabla(v-w)\|_{0,K}^2 = k^2 \|v\|_{0,K}^2 - k^2 \|w\|_{0,K}^2$ which implies

$$\|\nabla(v-w)\|_{0,K} \le k \|v\|_{0,K}. \tag{2.12}$$

Taking $b_1$ as test function in (2.11), we have

$$\begin{aligned}
\int_K v\, \overline{b_1} \,\mathrm{d}V &= -\int_K w\, \overline{b_1} \,\mathrm{d}V + \frac{1}{k^2} \int_K (\nabla v - \nabla w) \cdot \overline{\nabla b_1} \,\mathrm{d}V \\
&\overset{(2.10)}{\le} -\int_K w\, \overline{b_1} \,\mathrm{d}V + \|\nabla(v-w)\|_{0,K}\, h_K\, |K|^{1/2} \\
&\overset{(2.12)}{\le} -\int_K w\, \overline{b_1} \,\mathrm{d}V + k\, \|v\|_{0,K}\, h_K\, |K|^{1/2}.
\end{aligned} \tag{2.13}$$

Moreover, by taking $\xi = w$ in (2.11), we have

$$a^K(v,w) = \|w\|_{1,k,K}^2.$$

In order to conclude, we need to prove that $\|v\|_{1,k,K} \le \frac{1}{\beta(h_K k)} \|w\|_{1,k,K}$.

From the definition of $a^K(\cdot,\cdot)$ and from (2.11), setting $c_v = \frac{1}{|K|}\int_K v \,\mathrm{d}V$, we have

$$\begin{aligned}
\|v\|_{1,k,K}^2 = a^K(v,v) + 2k^2 \|v\|_{0,K}^2 &= \int_K \nabla w \cdot \overline{\nabla v} \,\mathrm{d}V + k^2 \int_K w\, \overline{v} \,\mathrm{d}V + 2k^2 \|v\|_{0,K}^2 \\
&\le \|w\|_{1,k,K} \|v\|_{1,k,K} + 2k^2 \|v - c_v\|_{0,K}^2 + 2k^2 \|c_v\|_{0,K}^2.
\end{aligned} \tag{2.14}$$

The min-max principle implies

$$\frac{\|\nabla v\|_{0,K}^2}{\|v - c_v\|_{0,K}^2} \ge \mu_2 \ge \frac{C_0\, \pi^2}{h_K^2} \qquad \Rightarrow \quad 2k^2 \|v - c_v\|_{0,K}^2 \le \left(\frac{\sqrt{2}\, h_K k}{\sqrt{C_0}\, \pi}\right)^2 \|\nabla v\|_{0,K}^2. \tag{2.15}$$

For the term $2k^2 \|c_v\|_{0,K}^2$, we have

$$\begin{aligned} k\|c_v\|_{0,K} &= \frac{k}{|K|^{1/2}}\left|\int_K v\,\mathrm{d}V\right| = \frac{k}{|K|^{1/2}}\left|\int_K v\,\overline{b_1}\,\mathrm{d}V + \int_K v\,(\overline{1-b_1})\,\mathrm{d}V\right| \\ &\overset{(2.13)}{\leq} \frac{k}{|K|^{1/2}}\left|\int_K w\,\overline{b_1}\,\mathrm{d}V\right| + (h_K k)k\|v\|_{0,K} + \frac{k}{|K|^{1/2}}\left|\int_K v\,(\overline{1-b_1})\,\mathrm{d}V\right| \\ &\leq \frac{k}{|K|^{1/2}}\|w\|_{0,K}\|b_1\|_{0,K} + (h_K k)k\|v\|_{0,K} + \frac{k}{|K|^{1/2}}\|v\|_{0,K}\|1-b_1\|_{0,K} \\ &\overset{(2.8),(2.9)}{\leq} k\|w\|_{0,K} + (h_K k)k\|v\|_{0,K} + \frac{(h_K k)^2}{2}k\|v\|_{0,K} \\ &= k\|w\|_{0,K} + \left[1+\frac{h_K k}{2}\right](h_K k)k\|v\|_{0,K}\,. \end{aligned} \tag{2.16}$$

Inserting (2.15) and (2.16) into (2.14) gives

$$\begin{aligned} \|v\|_{1,k,K}^2 &\leq \|w\|_{1,k,K}\|v\|_{1,k,K} + \left(\frac{\sqrt{2}\,h_K k}{\sqrt{C_0}\,\pi}\right)^2\|\nabla v\|_{0,K}^2 + 2k^2\|w\|_{0,K}^2 + 2\left[1+\frac{h_K k}{2}\right]^2(h_K k)^2 k^2\|v\|_{0,K}^2 \\ &\quad + 4\left[1+\frac{h_K k}{2}\right](h_K k)k\|w\|_{0,K}\,k\|v\|_{0,K} \\ &\leq \left(3+4(h_K k)+2(h_K k)^2\right)\|w\|_{1,k,K}\|v\|_{1,k,K} \\ &\quad + \max\left\{\left(\frac{\sqrt{2}\,h_K k}{\sqrt{C_0}\,\pi}\right)^2, 2\left[1+\frac{h_K k}{2}\right]^2(h_K k)^2\right\}\|v\|_{1,k,K}^2\,, \end{aligned}$$

where in the last step we also have used $k^2\|w\|_{0,K}^2 \leq k\|w\|_{0,K}\,k\|v\|_{0,K}$; thus

$$\frac{1-\max\left\{\left(\frac{\sqrt{2}\,h_K k}{\sqrt{C_0}\,\pi}\right)^2, 2\left[1+\frac{h_K k}{2}\right]^2(h_K k)^2\right\}}{3+4(h_K k)+2(h_K k)^2}\|v\|_{1,k,K} \leq \|w\|_{1,k,K}\,,$$

with a positive coefficient on the left-hand side, provided that $\max\left\{\left(\frac{\sqrt{2}\,h_K k}{\sqrt{C_0}\,\pi}\right)^2, 2\left[1+\frac{h_K k}{2}\right]^2(h_K k)^2\right\} < 1$, *i.e.*, provided that (2.6) is satisfied (whenever $K$ is convex, $C_0 = 1$, and the condition is $h_K k < 0.5538$). Then, (2.7) holds with

$$\beta(h_K k) = \frac{1-\max\left\{\left(\frac{\sqrt{2}\,h_K k}{\sqrt{C_0}\,\pi}\right)^2, 2\left[1+\frac{h_K k}{2}\right]^2(h_K k)^2\right\}}{3+4(h_K k)+2(h_K k)^2}.$$ □

**Remark 2.2.** In the infinite dimensional case, under the restriction $0 < h_K k \leq \alpha_1 < \frac{\sqrt{C_0}\,\pi}{\sqrt{2}}$, the following inf-sup condition holds true:

$$\forall v \in H^1(K) \quad \exists w \in H^1(K) \quad \text{s.t.} \quad \frac{a^K(v,w)}{\|w\|_{1,k,K}} \geq \beta^*(h_K k)\|v\|_{1,k,K}\,,$$

with $\beta^*(h_K k) = 1 - \left(\frac{\sqrt{2}\,h_K k}{\sqrt{C_0}\,\pi}\right)^2$. This can be proved along the same lines as in the proof of Proposition 2.1, choosing $b_1 \equiv 1$ since, in this case, it is an admissible test function.

We have carried out numerical tests in the convex case ($C_0 = 1$), in order to numerically determine the inf-sup constant in (2.7), with only the above restriction on the product $h_K k$. The results obtained seem to indicate

that the function $\beta$ is bounded from below by the function $\beta^*$, and thus that the stronger restriction (2.6) on $h_K k$ we have required in Proposition 2.1 might not be needed in practice.

The following result is a straightforward consequence of the inf-sup condition (2.7).

**Proposition 2.3.** *Under the condition (2.5), the operator $\Pi$ is well-defined, and the following local continuity continuity property holds true:*

$$\|\Pi u\|_{1,k,K} \leq \frac{1}{\beta(h_K k)} \|u\|_{1,k,K} \qquad \forall u \in V_p(K).$$

## 2.4. The matrices $D$, $B$, $G$, and $P$

With the same notation as [10], we introduce the basic components of our PW-VEM.

Let $D$ be the matrix of size $(n_K p, p)$ whose $\ell$th column contains the coefficients of the representation of the plane wave $\pi_\ell$ in the $V_p(K)$ basis $\{\psi_r\}$. Simple calculations, taking into account that $\{\varphi_j\}_{j=1}^{n_K}$ is a partition of unity, show that the only entries of $D$ different from zero are

$$D((j-1)p+\ell, \ell) = \mathrm{e}^{-ik\mathbf{d}_\ell \cdot (\mathbf{x}_K - \mathbf{x}_j)}, \qquad j = 1, \dots, n_K, \ \ell = 1, \dots, p.$$

We define $B$ as the matrix of dimension $(p, n_K p)$ such that

$$B(\ell, r) = a^K(\psi_r, \pi_\ell), \qquad \ell = 1, \dots, p, \ r = 1, \dots, n_K p.$$

As already observed in the definition of $\Pi$, since $\Delta \pi_\ell + k^2 \pi_\ell = 0$, the entries of $B$ can be computed in terms of the traces of the shape functions on $\partial K$ only:

$$\begin{aligned} B(\ell, r) = a^K(\psi_r, \pi_\ell) &= \int_K \nabla \psi_r \cdot \overline{\nabla \pi_\ell} \, \mathrm{d}V - k^2 \int_K \psi_r \, \overline{\pi}_\ell \, \mathrm{d}V \\ &= \int_{\partial K} \psi_r \, \overline{\nabla \pi_\ell} \cdot \boldsymbol{\nu}_K \, \mathrm{d}S = -ik \int_{\partial K} \mathbf{d}_\ell \cdot \boldsymbol{\nu}_K \, \psi_r \, \overline{\pi}_\ell \, \mathrm{d}S, \end{aligned}$$

where we have used $\overline{\nabla \pi_\ell} = -ik \, \mathbf{d}_\ell \, \overline{\pi}_\ell$. The integral defining $B(\ell, r)$ can be computed exactly, as shown in Remark 2.5 below.

Finally, $G$ is the matrix of size $(p, p)$ defined by

$$G(\ell, m) = a^K(\pi_m, \pi_\ell), \qquad m, \ell = 1, \dots, p.$$

The matrix $G$ is Hermitian and invertible, provided that $h_K k$ is sufficiently small (see (2.5)). The matrix $G$ can be expressed in terms of $B$ and $D$ as

$$G = BD.$$

Actually, $G$ can be computed directly, without using quadrature formulae (see Rem. 2.5 below). $B$ and $D$ have to be computed in any case.

The matrix representation of the operator $\Pi$ is $G^{-1}B$, thus the matrix $P$ of size $(n_K p, n_K p)$ defined by

$$P = DG^{-1}B$$

is the matrix representation of the composition of the inclusion of $V_{p_K}^*(K)$ in $V_{p_K}(K)$ after $\Pi$.

### 2.5. The local PW-VEM bilinear form

Following the VEM paradigm, we split the local bilinear form $a^K(u,v)$ in a part that can be computed exactly (up to machine precision), and in a part that can be suitably approximated, provided that some stability properties are satisfied. Indeed, by using the projector $\Pi$, the local bilinear form can be written as

$$a^K(u,v) = a^K(\Pi u, \Pi v) + a^K((I-\Pi)u, (I-\Pi)v).$$

The term $a^K(\Pi u, \Pi v)$ can be computed in terms of the traces of the shape functions on $\partial K$ only. Its matrix representation $A_\Pi$ is

$$A_\Pi = \overline{B}^T \, \overline{G}^{-1} B.$$

On the contrary, the computation of the term $a^K((I-\Pi)u, (I-\Pi)v)$ would require values of all the shape functions in the interior of $K$ and it will be approximated (see Sect. 4 below). We denote its approximation by $s^K((I-\Pi)u, (I-\Pi)v)$, and the local PW-VEM bilinear form can be written as

$$a_h^K(u,v) = a^K(\Pi u, \Pi v) + s^K((I-\Pi)u, (I-\Pi)v).$$

Since $\Pi u_p^* = u_p^*$ for all $u_p^* \in V_p^*(K)$, the following *plane wave-consistency* property holds true:

$$a_h^K(u_p^*, v) = a^K(u_p^*, v) \qquad \forall u_p^* \in V_p^*(K),\ v \in V_p(K). \tag{2.17}$$

### 2.6. The global PW-VEM formulation

The global bilinear form defining the PW-VEM method is given by

$$b_h(u,v) = a_h(u,v) + ik \int_{\partial\Omega} u\overline{v} \, \mathrm{d}S, \tag{2.18}$$

where

$$a_h(u,v) = \sum_{K\in\mathcal{T}_h} a_h^K(u,v) = \sum_{K\in\mathcal{T}_h} \left[ a^K(\Pi u, \Pi v) + s^K((I-\Pi)u, (I-\Pi)v) \right],$$

with $s^K(\cdot,\cdot)$ to be defined. Thus, the methods reads: find $u_{hp} \in V_p(\mathcal{T}_h)$ such that

$$b_h(u_{hp}, v) = \int_{\partial\Omega} g\overline{v} \, \mathrm{d}S \qquad \forall v \in V_p(\mathcal{T}_h). \tag{2.19}$$

The boundary integral on the right-hand side of equation (2.18) is computed exactly (see Rem. 2.5 below), thus the only integral which requires quadrature is the boundary integral on the right-hand side of (2.19), containing the inhomogeneous boundary datum. In our theoretical analysis, nevertheless, in order to avoid complications, we assume that also this integral is computed exactly.

**Remark 2.4.** We point out that the *plane wave-consistency* property (2.17) and the definition of $a_h(.,.)$ imply that the *Patch Test* is satisfied, in the following sense. On any patch of elements, if the exact solution is a plane wave in one of the $\mathbf{d}_\ell$ directions that define the local spaces $V_p^*(K)$ (or a linear combination of such plane waves), then the exact solution and the approximate solution coincide.

**Remark 2.5.** The computation of volume and edge integrals of products of plane waves, as well as that of edge integrals of products of plane waves by polynomial functions, can be done exactly (see [25] and [27], pp. 20–21).

In fact, if $F$ is a mesh face (edge), denoting by $\mathbf{a}$ and $\mathbf{b}$ the coordinate vector of its endpoints, we have

$$\begin{aligned} \int_F \mathrm{e}^{ik(\mathbf{d}_m - \mathbf{d}_\ell)\cdot\mathbf{x}} \, \mathrm{d}S &= |F| \mathrm{e}^{ik(\mathbf{d}_m - \mathbf{d}_\ell)\cdot\mathbf{a}} \int_0^1 \mathrm{e}^{ik(\mathbf{d}_m - \mathbf{d}_\ell)\cdot(\mathbf{b}-\mathbf{a})t} \, \mathrm{d}t \\ &= |F| \mathrm{e}^{ik(\mathbf{d}_m - \mathbf{d}_\ell)\cdot\mathbf{a}} \Phi_1\big(ik(\mathbf{d}_m - \mathbf{d}_\ell)\cdot(\mathbf{b}-\mathbf{a})\big), \end{aligned}$$

where $|F|$ denotes the length of $F$ and, for $z \in \mathbb{C}$,

$$\Phi_1(z) = \int_0^1 \mathrm{e}^{zt}\,\mathrm{d}t = \begin{cases} \dfrac{\mathrm{e}^z - 1}{z} & \text{if } z \neq 0 \\ 1 & \text{if } z = 0. \end{cases}$$

This formula also enters the computation of plane wave mass matrices, whose entries are integrals of the type

$$\int_K \mathrm{e}^{ik(\mathbf{d}_m - \mathbf{d}_\ell)\cdot\mathbf{x}}\,\mathrm{d}V.$$

For $m = \ell$, this integral is simply $|K|$, the area of $K$. Whenever $m \neq \ell$, using $\Delta \mathrm{e}^{ik\mathbf{d}\cdot\mathbf{x}} = -k^2\mathbf{d}\cdot\mathbf{d}\,\mathrm{e}^{ik\mathbf{d}\cdot\mathbf{x}}$, one has

$$\int_K \mathrm{e}^{ik(\mathbf{d}_m - \mathbf{d}_\ell)\cdot\mathbf{x}}\,\mathrm{d}V = \sum_{F\in\partial K} \frac{(\mathbf{d}_m - \mathbf{d}_\ell)\cdot\mathbf{n}_F}{ik(\mathbf{d}_m - \mathbf{d}_\ell)\cdot(\mathbf{d}_m - \mathbf{d}_\ell)} \int_F \mathrm{e}^{ik(\mathbf{d}_m - \mathbf{d}_\ell)\cdot\mathbf{x}}\,\mathrm{d}S,$$

where $\mathbf{n}_F$ is the normal unit vector to $F$ pointing outside $K$.

For the matrix $B$, we have seen that $B(\ell, r) = -ik\int_{\partial K} \mathbf{d}_\ell\cdot\boldsymbol{\nu}_K\,\psi_r\,\overline{\pi}_\ell\,\mathrm{d}S$. Thus, we need to compute integrals of the type

$$\int_F \varphi_j(\mathbf{x})\mathrm{e}^{ik(\mathbf{d}_m - \mathbf{d}_\ell)\cdot\mathbf{x}}\,\mathrm{d}S.$$

If $V_j$ is not an endpoint of $F$, then this integral is zero. Otherwise, denoting by $\mathbf{a}$ the coordinate vector of $V_j$ and by $\mathbf{b}$ the coordinate vector of the other endpoint of $F$, we have

$$\begin{aligned}\int_F \varphi_j(\mathbf{x})\mathrm{e}^{ik(\mathbf{d}_m - \mathbf{d}_\ell)\cdot\mathbf{x}}\,\mathrm{d}S &= |F|\mathrm{e}^{ik(\mathbf{d}_m - \mathbf{d}_\ell)\cdot\mathbf{a}} \int_0^1 (1-t)\mathrm{e}^{ik(\mathbf{d}_m - \mathbf{d}_\ell)\cdot(\mathbf{b}-\mathbf{a})t}\,\mathrm{d}t \\ &= |F|\mathrm{e}^{ik(\mathbf{d}_m - \mathbf{d}_\ell)\cdot\mathbf{a}}\,\Phi_2\big(ik(\mathbf{d}_m - \mathbf{d}_\ell)\cdot(\mathbf{b}-\mathbf{a})\big),\end{aligned}$$

where

$$\Phi_2(z) = \int_0^1 (1-t)\mathrm{e}^{zt}\,dt = \begin{cases} \dfrac{\mathrm{e}^z - z - 1}{z^2} & \text{if } z \neq 0 \\ 1/2 & \text{if } z = 0. \end{cases}$$

Similarly, for the integral on the right-hand side of (2.18), we have to compute integrals of the type

$$\int_F \varphi_i(\mathbf{x})\varphi_j(\mathbf{x})\mathrm{e}^{ik(\mathbf{d}_m - \mathbf{d}_\ell)\cdot\mathbf{x}}\,\mathrm{d}S.$$

Whenever either $V_i$ or $V_j$ is not an endpoint of $F$, the integral is zero. Otherwise, we distinguish two cases. If $i = j$, denoting by $\mathbf{a}$ the coordinate vector of $V_i = V_j$ and by $\mathbf{b}$ the coordinate vector of the other endpoint of $F$, we have

$$\begin{aligned}\int_F \varphi_i(\mathbf{x})\varphi_j(\mathbf{x})\mathrm{e}^{ik(\mathbf{d}_m - \mathbf{d}_\ell)\cdot\mathbf{x}}\,\mathrm{d}S &= |F|\mathrm{e}^{ik(\mathbf{d}_m - \mathbf{d}_\ell)\cdot\mathbf{a}} \int_0^1 (1-t)^2\mathrm{e}^{ik(\mathbf{d}_m - \mathbf{d}_\ell)\cdot(\mathbf{b}-\mathbf{a})t}\,\mathrm{d}t \\ &= |F|\mathrm{e}^{ik(\mathbf{d}_m - \mathbf{d}_\ell)\cdot\mathbf{a}}\,\Phi_3\big(ik(\mathbf{d}_m - \mathbf{d}_\ell)\cdot(\mathbf{b}-\mathbf{a})\big),\end{aligned}$$

where

$$\Phi_3(z) = \int_0^1 (1-t)^2\mathrm{e}^{zt}\,\mathrm{d}t = \begin{cases} \dfrac{2(\mathrm{e}^z - z - 1) - z^2}{z^3} & \text{if } z \neq 0 \\ 1/3 & \text{if } z = 0. \end{cases}$$

In the second case, when $i \neq j$, denoting by $\mathbf{a}$ and $\mathbf{b}$ the coordinate vector of $V_j$ and $V_i$ respectively, we have

$$\begin{aligned}\int_F \varphi_i(\mathbf{x})\varphi_j(\mathbf{x})\mathrm{e}^{ik(\mathbf{d}_m-\mathbf{d}_\ell)\cdot\mathbf{x}}\,\mathrm{d}S &= |F|\mathrm{e}^{ik(\mathbf{d}_m-\mathbf{d}_\ell)\cdot\mathbf{a}}\int_0^1 (1-t)t\,\mathrm{e}^{ik(\mathbf{d}_m-\mathbf{d}_\ell)\cdot(\mathbf{b}-\mathbf{a})t}\,\mathrm{d}t\\ &= |F|\mathrm{e}^{ik(\mathbf{d}_m-\mathbf{d}_\ell)\cdot\mathbf{a}}\Phi_4\big(ik(\mathbf{d}_m-\mathbf{d}_\ell)\cdot(\mathbf{b}-\mathbf{a})\big),\end{aligned}$$

where

$$\Phi_4(z) = \int_0^1 (1-t)t\mathrm{e}^{zt}\,\mathrm{d}t = \begin{cases}\dfrac{\mathrm{e}^z(z-2)+z+2}{z^3} & \text{if } z\neq 0\\ 1/6 & \text{if } z=0.\end{cases}$$

## 3. Analysis

The last step in defining our discretization scheme is the choice of the stabilization term $s^K((I-\Pi)u,(I-\Pi)v)$. Before doing so, we first pose some abstract properties on the discrete problem that provide convergence results.

### 3.1. Abstract result

Let us introduce the $k$-dependent norm for functions in $H^1(\Omega)$:

$$\|v\|^2_{1,k,\Omega} = \|\nabla v\|^2_{0,\Omega} + k^2\|v\|^2_{0,\Omega},$$

and the corresponding broken norm

$$\|v\|^2_{1,k,\mathcal{T}_h} = \sum_{K\in\mathcal{T}_h}\|v\|^2_{1,k,K} = \sum_{K\in\mathcal{T}_h}(\|\nabla v\|^2_{0,K} + k^2\|v\|^2_{0,K}),$$

defined in the space $H^1(\mathcal{T}_h)$ of broken $H^1$-functions.

The continuous bilinear form $b(\cdot,\cdot)$ satisfies the following continuity (see [38], Lem. 8.1.6) and Gårding inequality

$$\begin{aligned}|b(u,v)| &\le C_{\mathrm{cont}}\|u\|_{1,k,\Omega}\|v\|_{1,k,\Omega},\\ \mathrm{Re}[b(v,v)] + 2k^2\|v\|^2_{0,\Omega} &= \|v\|^2_{1,k,\Omega}\end{aligned}$$

for all $u,v\in H^1(\Omega)$.

Since for functions in $H^1(\Omega)$ the $\|\cdot\|_{1,k,\Omega}$-norm and the $\|\cdot\|_{1,k,\mathcal{T}_h}$-norm coincide, from here on, we will write $\|\cdot\|_{1,k,\mathcal{T}_h}$ for both, whenever convenient.

**Theorem 3.1.** *Assume that the local stabilization forms $s^K(\cdot,\cdot)$ are chosen in such a way that the following properties hold true:*

- continuity*: there exists $\gamma>0$ such that, for all $u,v\in H^1(\mathcal{T}_h)$,*

$$|a_h(u,v)| \le \gamma\|u\|_{1,k,\mathcal{T}_h}\|v\|_{1,k,\mathcal{T}_h}; \tag{3.1}$$

- Gårding inequality for the discrete operator*: there exists $\alpha>0$ such that*

$$Re[b_h(v,v)] + 2k^2\|v\|^2_{0,\Omega} \ge \alpha\|v\|^2_{1,k,\mathcal{T}_h} \qquad \forall v\in V_p(\mathcal{T}_h). \tag{3.2}$$

*Let $u$ be the solution to problem (2.2), and let $u_{hp}$ be solution to the PW-VEM method (2.19) in $V_p(\mathcal{T}_h)$. Then, provided that $h$ is small enough with respect to $k$ (see (3.13) below), the following error estimate holds:*

$$\|u-u_{hp}\|_{1,k,\mathcal{T}_h} \le C\frac{1+\alpha+\gamma}{\alpha}\left(\inf_{v_I\in V_p(\mathcal{T}_h)}\|u-v_I\|_{1,k,\mathcal{T}_h} + \inf_{v^*_{hp}\in V^*_p(\mathcal{T}_h)}\|u-v^*_{hp}\|_{1,k,\mathcal{T}_h}\right),$$

*with $C>0$ independent on $h$, $k$ and $p$. Well-posedness of the PW-VEM method directly follows.*

*Proof.* By the triangle inequality, we have

$$\|u-u_{hp}\|_{1,k,\mathcal{T}_h} \le \|u-v_I\|_{1,k,\mathcal{T}_h} + \|v_I-u_{hp}\|_{1,k,\mathcal{T}_h}\,, \tag{3.3}$$

for any $v_I \in V_p(\mathcal{T}_h)$. We set $\delta_{hp} = u_{hp} - v_I$, and proceed by estimating $\|\delta_{hp}\|_{1,k,\mathcal{T}_h}$.

The Gårding inequality (3.2) gives

$$\alpha\,\|\delta_{hp}\|^2_{1,k,\mathcal{T}_h} \le \mathrm{Re}[b_h(\delta_{hp},\delta_{hp})] + 2k^2\,\|\delta_{hp}\|^2_{0,\Omega} =: \; I \,+\, II. \tag{3.4}$$

The term $I$ can be treated as in Theorem 3.1 of [5]. Using the definition of $b_h(\cdot,\cdot)$ and the discrete equation (2.19), for any $v^*_{hp}$ in $V^*_p(\mathcal{T}_h)$, we get

$$\begin{aligned}
b_h(\delta_{hp},\delta_{hp}) &= b_h(u_{hp},\delta_{hp}) - a_h(v_I,\delta_{hp}) - ik\int_{\partial\Omega} v_I\overline{\delta}_{hp}\,\mathrm{d}S \\
&= \int_{\partial\Omega} g\overline{\delta}_{hp}\,\mathrm{d}S - \sum_{K\in\mathcal{T}_h} a^K_h(v_I,\delta_{hp}) - ik\int_{\partial\Omega} v_I\overline{\delta}_{hp}\,\mathrm{d}S \quad \text{(insert } v^*_{hp} \text{ and use } \textit{pw-consist.}\ (2.17))\\
&= \int_{\partial\Omega} g\overline{\delta}_{hp}\,\mathrm{d}S - \sum_{K\in\mathcal{T}_h} a^K_h(v_I-v^*_{hp},\delta_{hp}) - \sum_{K\in\mathcal{T}_h} a^K(v^*_{hp},\delta_{hp}) - ik\int_{\partial\Omega} v_I\overline{\delta}_{hp}\,\mathrm{d}S \quad \text{(use (2.2))}\\
&= a(u,\delta_{hp}) + ik\int_{\partial\Omega} u\,\overline{\delta}_{hp}\,\mathrm{d}S - a_h(v_I-v^*_{hp},\delta_{hp}) - \sum_{K\in\mathcal{T}_h} a^K(v^*_{hp},\delta_{hp}) - ik\int_{\partial\Omega} v_I\overline{\delta}_{hp}\,\mathrm{d}S\\
&= \sum_{K\in\mathcal{T}_h} a^K(u-v^*_{hp},\delta_{hp}) + a_h(v^*_{hp}-v_I,\delta_{hp}) + ik\int_{\partial\Omega}(u-v_I)\overline{\delta}_{hp}\,\mathrm{d}S.
\end{aligned} \tag{3.5}$$

In order to bound the last term, we observe that the trace inequality states that there exists a constant $C>0$ only depending on the shape of $\Omega$ such that, for all $v\in H^1(\Omega)$,

$$\begin{aligned}
k^{1/2}\,\|v\|_{0,\partial\Omega} &\le Ck^{1/2}\left(\mathrm{diam}(\Omega)^{-1/2}\,\|v\|_{0,\Omega} + \|v\|^{1/2}_{0,\Omega}\,\|\nabla v\|^{1/2}_{0,\Omega}\right)\\
&\le C\left[k^{-1/2}\,\mathrm{diam}(\Omega)^{-1/2}\,\|v\|_{1,k,\Omega} + \left(\frac{k}{2}\,\|v\|_{0,\Omega} + \frac{1}{2}\,\|\nabla v\|_{0,\Omega}\right)\right]\\
&\le C\left(\mathrm{diam}(\Omega)^{-1/2}k^{-1/2}\,\|v\|_{1,k,\Omega} + \|v\|_{1,k,\Omega}\right).
\end{aligned}$$

Due to the high-frequency assumption, it holds $k^{-1}\,\mathrm{diam}(\Omega)^{-1} < 1/2\pi$, and we conclude that there exists a constant $C>0$ only depending on $\Omega$ such that, for all $v\in H^1(\Omega)$,

$$k^{1/2}\,\|v\|_{0,\partial\Omega} \le C\,\|v\|_{1,k,\Omega}\,.$$

Thus, since both $(u-v_I)$ and $\delta_{hp}$ belong to $H^1(\Omega)$, we have

$$\begin{aligned}
\left|ik\int_{\partial\Omega}(u-v_I)\overline{\delta}_{hp}\,\mathrm{d}S\right| &\le k\,\|u-v_I\|_{0,\partial\Omega}\,\|\delta_{hp}\|_{0,\partial\Omega}\\
&\le C\,\|u-v_I\|_{1,k,\Omega}\,\|\delta_{hp}\|_{1,k,\Omega}\,,
\end{aligned} \tag{3.6}$$

with a constant $C>0$ only depending on $\Omega$.

From (3.5) and (3.6), using the continuity of the bilinear form and the continuity property (3.1), we can conclude with the following estimate of the term $I$:

$$I = \mathrm{Re}[b_h(\delta_{hp},\delta_{hp})] \le C_I(1+\gamma)\left(\left\|u-v^*_{hp}\right\|_{1,k,\mathcal{T}_h} + \|u-v_I\|_{1,k,\mathcal{T}_h}\right)\|\delta_{hp}\|_{1,k,\mathcal{T}_h}\,.$$

For the term $II$, we have

$$\begin{aligned} II = 2k^2 \|\delta_{hp}\|_{0,\Omega}^2 &\le 2k^2 \|\delta_{hp}\|_{0,\Omega} (\|u-u_{hp}\|_{0,\Omega} + \|u-v_I\|_{0,\Omega}) \\ &\le 2k \|\delta_{hp}\|_{1,k,\mathcal{T}_h} (\|u-u_{hp}\|_{0,\Omega} + \|u-v_I\|_{0,\Omega}), \end{aligned}$$

due to $k\|\delta_{hp}\|_{0,\Omega} \le \|\delta_{hp}\|_{1,k,\mathcal{T}_h}$. Inserting the bounds for $I$ and $II$ into (3.4) gives

$$\begin{aligned} \alpha \|\delta_{hp}\|_{1,k,\mathcal{T}_h} &\le C_I(1+\gamma)(\|u-v_{hp}^*\|_{1,k,\mathcal{T}_h} + \|u-v_I\|_{1,k,\mathcal{T}_h}) + 2k(\|u-u_{hp}\|_{0,\Omega} + \|u-v_I\|_{0,\Omega}) \\ &\le C_{II}(1+\gamma)(\|u-v_{hp}^*\|_{1,k,\mathcal{T}_h} + \|u-v_I\|_{1,k,\mathcal{T}_h}) + 2k\|u-u_{hp}\|_{0,\Omega}, \end{aligned} \tag{3.7}$$

where we have used again $k\|u-v_I\|_{0,\Omega} \le \|u-v_I\|_{1,k,\mathcal{T}_h}$.

The term $\|u-u_{hp}\|_{0,\Omega}$ can be estimated by using a duality argument. Let us denote by $\psi$ the solution of the dual problem

$$b(v,\psi) = \int_\Omega v\,\overline{(u-u_{hp})}\,\mathrm{d}V \qquad \forall v \in H^1(\Omega). \tag{3.8}$$

Since $\Omega$ is assumed to be convex, $\psi$ belongs to $H^2(\Omega)$ and satisfies

$$\begin{aligned} &\|\psi\|_{1,k,\mathcal{T}_h} \le C\|u-u_{hp}\|_{0,\Omega}, \\ &|\psi|_{2,\Omega} \le C(1+k)\|u-u_{hp}\|_{0,\Omega}; \end{aligned} \tag{3.9}$$

see Proposition 8.1.4 of [38].

In correspondence to $\psi \in H^2(\Omega)$, there exist $\psi_{hp}^* \in V_p^*(\mathcal{T}_h)$ and $\psi_I \in V_p(\mathcal{T}_h)$ and $\psi_I \in V_p(\mathcal{T}_h)$ such that

$$\begin{aligned} \|\psi-\psi_{hp}^*\|_{1,k,\mathcal{T}_h} &\le C(1+hk)\,h\,\|\psi\|_{2,k,\Omega}, \\ \|\psi-\psi_I\|_{1,k,\mathcal{T}_h} &\le C(1+hk)\,h\,\|\psi\|_{2,k,\Omega}, \end{aligned} \tag{3.10}$$

with $C>0$ independent of $h$, $k$ and $\psi$. The first bound follows as in Propositions 3.12 and 3.13 of [28]. The second one follows from combining Theorem 2.1 of [39] with the local approximation estimates in plane wave spaces (the harmonic functions $\varphi_j$ on $K$ form a partition of unity and satisfy $\|\varphi_j\|_{L^\infty(K)} \le C$, by the maximum principle, and $\|\nabla\varphi_j\|_{L^\infty(K)^2} \le C/h_K$, due to the convexity of $K$ and the assumption of non degenerating sides).

Using (3.8) with $v = u-u_{hp}$, and inserting $\psi_I$, we have

$$\begin{aligned} \|u-u_{hp}\|_{0,\Omega}^2 &= b(u-u_{hp},\psi) = b(u-u_{hp},\psi-\psi_I) + b(u-u_{hp},\psi_I) \\ &\overset{(2.2),(2.19)}{=} b(u-u_{hp},\psi-\psi_I) + \int_{\partial\Omega} g\overline{\psi}_I\,\mathrm{d}S - b(u_{hp},\psi_I) \\ &\quad + b_h(u_{hp},\psi_I) - \int_{\partial\Omega} g\overline{\psi}_I\,\mathrm{d}S \\ &= b(u-u_{hp},\psi-\psi_I) - a(u_{hp},\psi_I) - ik\int_{\partial\Omega} u_{hp}\overline{\psi}_I\,\mathrm{d}S \\ &\quad + a_h(u_{hp},\psi_I) + ik\int_{\partial\Omega} u_{hp}\overline{\psi}_I\,\mathrm{d}S \\ &= b(u-u_{hp},\psi-\psi_I) + (a_h(u_{hp},\psi_I) - a(u_{hp},\psi_I)) =: III + IV. \end{aligned}$$

The term $III$ is bounded using the continuity of the continuous form $b(\cdot,\cdot)$, the second estimate in (3.10) and the regularity bounds (3.9):

$$\begin{aligned} III = b(u-u_{hp},\psi-\psi_I) &\le C\|u-u_{hp}\|_{1,k,\mathcal{T}_h}\|\psi-\psi_I\|_{1,k,\Omega} \\ &\le C_{III}\,(1+hk)\,h\,(1+k)\,\|u-u_{hp}\|_{1,k,\mathcal{T}_h}\|u-u_{hp}\|_{0,\Omega}. \end{aligned}$$

For the term $IV$, using the *pw-consistency* property (2.17) and the continuity of the discrete forms, we obtain

$$\begin{aligned} IV &= a_h(u_{hp},\psi_I) - a(u_{hp},\psi_I) = \sum_{K\in\mathcal{T}_h} (a_h^K(u_{hp},\psi_I) - a^K(u_{hp},\psi_I)) \\ &= \sum_{K\in\mathcal{T}_h} (a_h^K(u_{hp}-v_{hp}^*,\psi_I) - a^K(u_{hp}-v_{hp}^*,\psi_I)) \\ &= \sum_{K\in\mathcal{T}_h} (a_h^K(u_{hp}-v_{hp}^*,\psi_I-\psi_{hp}^*) - a^K(u_{hp}-v_{hp}^*,\psi_I-\psi_{hp}^*)) \\ &\le (1+\gamma)\left\|u_{hp}-v_{hp}^*\right\|_{1,k,\mathcal{T}_h}\left\|\psi_I-\psi_{hp}^*\right\|_{1,k,\mathcal{T}_h}. \end{aligned} \tag{3.11}$$

Next, using the bounds in (3.10) and (3.9), we have

$$\begin{aligned} \left\|\psi_I-\psi_{hp}^*\right\|_{1,k,\mathcal{T}_h} &\le \|\psi_I-\psi\|_{1,k,\mathcal{T}_h} + \left\|\psi-\psi_{hp}^*\right\|_{1,k,\mathcal{T}_h} \\ &\le C\,(1+hk)\,h\,(1+k)\;\|u-u_{hp}\|_{0,\Omega}, \end{aligned}$$

that we insert in (3.11) getting

$$IV \le C_{IV}\,(1+\gamma)\,(1+hk)\,h\,(1+k)\,(\|u-u_{hp}\|_{1,k,\mathcal{T}_h} + \left\|u-v_{hp}^*\right\|_{1,k,\mathcal{T}_h})\,\|u-u_{hp}\|_{0,\Omega}.$$

Therefore, we conclude with the following bound for $\|u-u_{hp}\|_{0,\Omega}$:

$$\|u-u_{hp}\|_{0,\Omega} \le (C_{III}+C_{IV})\,(1+\gamma)\,(1+hk)\,h\,(1+k)\,(\|u-u_{hp}\|_{1,k,\mathcal{T}_h} + \left\|u-v_{hp}^*\right\|_{1,k,\mathcal{T}_h}), \tag{3.12}$$

which, inserted into (3.7), gives

$$\begin{aligned} \alpha\,\|\delta_{hp}\|_{1,k,\mathcal{T}_h} &\le C_{II}\,(1+\gamma)(\left\|u-v_{hp}^*\right\|_{1,k,\mathcal{T}_h} + \|u-v_I\|_{1,k,\mathcal{T}_h}) \\ &\quad + C_{\mathrm{dual}}\,(1+\gamma)\,k\,(1+hk)\,h\,(1+k)\,(\|u-u_{hp}\|_{1,k,\mathcal{T}_h} + \left\|u-v_{hp}^*\right\|_{1,k,\mathcal{T}_h}), \end{aligned}$$

($C_{\mathrm{dual}} = 2(C_{III}+C_{IV})$) and thus, owing to (3.3),

$$\begin{aligned} \alpha\,\|u-u_{hp}\|_{1,k,\mathcal{T}_h} &\le C_{II}\,(1+\alpha+\gamma)(\left\|u-v_{hp}^*\right\|_{1,k,\mathcal{T}_h} + \|u-v_I\|_{1,k,\mathcal{T}_h}) \\ &\quad + C_{\mathrm{dual}}\,(1+\gamma)\,k\,(1+hk)\,h\,(1+k)\,(\|u-u_{hp}\|_{1,k,\mathcal{T}_h} + \left\|u-v_{hp}^*\right\|_{1,k,\mathcal{T}_h}). \end{aligned}$$

Under the assumption

$$C_{\mathrm{dual}}\,(1+\gamma)\,(1+hk)\,hk\,(1+k) \le \frac{\alpha}{2}, \tag{3.13}$$

we can take the $\|u-u_h\|_{1,k,\mathcal{T}_h}$ term to the left-hand side and obtain

$$\|u-u_{hp}\|_{1,k,\mathcal{T}_h} \le C\,\frac{1+\alpha+\gamma}{\alpha}\,(\left\|u-v_{hp}^*\right\|_{1,k,\mathcal{T}_h} + \|u-v_I\|_{1,k,\mathcal{T}_h}),$$

with $C = 2C_{II}+1$, which completes the proof. □

**Remark 3.2.** From (3.13), it is clear that the threshold condition on $h$ required in Theorem 3.1 is that $(1+hk)\,hk\,(1+k)$ be sufficiently small, which, in the relevant case of large $k$, is equivalent to requiring that $hk^2$ be sufficiently small. This reflects the *pollution effect* of the $h$-version of the PW-VEM [3]. In fact, while a condition on $hk$ is enough for the convergence of the best approximation (see Prop. 3.3 below), a stronger condition (namely, on $hk^2$) is required for the convergence of the method.

### 3.2. Convergence rates

The abstract convergence result of Theorem 3.1, combined with best approximation estimates of Helmholtz solutions within $V_p(\mathcal{T}_h)$ and $V_p^*(\mathcal{T}_h)$, gives convergence rates.

In order to state the following results, we define the weighted norm

$$\|u\|_{s,k,\Omega}^2 = \sum_{j=0}^{s} k^{2(s-j)} \, |u|_{j,\Omega}^2 \,,$$

where $|\cdot|_{j,\Omega}$ denotes the standard seminorm in $H^j(\Omega)$.

**Proposition 3.3.** *Let $u$ be a function in $H^{\ell+1}(\Omega)$, $\ell \geq 0$, such that $\Delta u + k^2 u = 0$ in $\Omega$. Then there exist $u_{hp}^* \in V_p^*(\mathcal{T}_h)$ and $u_I \in V_p(\mathcal{T}_h)$, with $p = 2m+1$, such that*

$$\left\|u - u_{hp}^*\right\|_{1,k,\mathcal{T}_h} \leq C\,\eta(hk)\,h^{\min\{m,\ell\}}\,\|u\|_{\min\{m,\ell\}+1,k,\Omega}\,,$$
$$\|u - u_I\|_{1,k,\mathcal{T}_h} \leq C\,\eta(hk)\,h^{\min\{m,\ell\}}\,\|u\|_{\min\{m,\ell\}+1,k,\Omega}\,,$$

*with $C > 0$ independent of $h$, $k$ and $u$ and*

$$\eta(hk) = \left(1 + (hk)^{m+9}\right) \mathrm{e}^{\left(\frac{7}{4} - \frac{3}{4}\rho\right)hk}.$$

*Proof.* The first bound follows from the local approximation estimates in plane wave spaces of ([29], Thm. 3.2.2) (see also [43] p. 831 and [42]). The second bound can be obtained from the local approximation estimates in plane wave spaces by Theorem 2.1 of [39]. □

Theorem 3.1 and Proposition 3.3 immediately give the following convergence result.

**Corollary 3.4.** *Under the assumptions of Theorem 3.1, if the solution $u$ to problem (2.2) belongs to $H^{\ell+1}(\Omega)$, $\ell \geq 1$, then, provided that the threshold condition (3.13) is satisfied, the following error estimate holds:*

$$\|u - u_{hp}\|_{1,k,\mathcal{T}_h} \leq C\,\frac{1+\alpha+\gamma}{\alpha}\,\eta(hk)\,h^{\min\{m,\ell\}}\,\|u\|_{\min\{m,\ell\}+1,k,\Omega}\,,$$

*with $C > 0$ independent on $h$, $k$ and $p = 2m+1$, and $\eta(hk)$ as in Proposition 3.3.*

**Remark 3.5.** For the validity of approximation estimates in plane wave spaces, the assumption of convexity of the mesh elements is not needed. It would be enough to assume that there exist $\rho \in (0, 1/2]$ and $0 < \rho_0 < \rho$ such that every $K \in \mathcal{T}_h$ contains a ball of radius $\rho h_K$ and is star-shaped with respect to a ball of radius $\rho_0 h_K$ and the same center, say $\mathbf{x}_0$ (see [42, 43]).

In order to extend our analysis of the PW-VEM to such elements, we should modify the definition of the VEM space. Indeed, provided that the VEM space admits a basis $\{\varphi_j\}_{j=1}^{n_K}$ which forms a partition of unity, $\varphi_j(V_i) = \delta_{ij}$, and $\varphi_j$ is linear along each edge of $K$, the defintion of our PW-VEM remains unchanged (the condition that the functions $\varphi_j$ are harmonic was never used in the design of the PW-VEM). If, in addition, the functions $\varphi_j$ are such that $\|\varphi_j\|_{L^\infty(K)} \leq C$ and $\|\nabla\varphi_j\|_{L^\infty(K)^2} \leq C/h_K$, then Theorem 2.1 of [39] applies, and also our analysis remains valid. The assumption of non degenerating sides is necessary.

This is a possible alternative definition of the VEM space which works in the above described situation. Let $K \in \mathcal{T}_h$ and consider its partition into the $n_K$ triangles obtained by connecting $\mathbf{x}_0$ with the $n_K$ vertices of $K$. Let $w_j$ be the piecewise linear function on this partition such that $w_j(V_i) = \delta_{ij}$ and $w_j(\mathbf{x}_0) = 1$. Then, we define the VEM space as $V(K) = \mathrm{span}\{\varphi_j,\ 1 \leq j \leq n_K\}$, with

$$\varphi_j(\mathbf{x}) = \frac{w_j(\mathbf{x})}{\sum_{\ell=1}^{n_K} w_\ell(\mathbf{x})} \qquad \forall \mathbf{x} \in K.$$

We stress once again that the explicit expression of the functions $\varphi_j$ in the element interiors is not needed for the design of the PW-VEM method. Also for the theoretical analysis, what matters is only the *existence* of a basis with the required properties.

## 4. Stabilization term

Let us give a sufficient condition on the stabilization term $s^K((I-\Pi)u,(I-\Pi)v))$ in order to guarantee the Gårding's inequality for the discrete operator. To this aim, we first state the following lemma.

**Lemma 4.1.** *For $u \in V_p(K)$, we have*

$$k^2 \int_K (u-\Pi u)\,\overline{w}\,\mathrm{d}V = \int_K \nabla(u-\Pi u)\cdot\overline{\nabla w}\,\mathrm{d}V \qquad \forall w \in V_p^*(K).$$

*Proof.* The explicit form of the bilinear form that defines the projector $\Pi$ (see (2.4)) gives, for all $w \in V_p^*(K)$,

$$\int_K \nabla\Pi u\cdot\overline{\nabla w}\,\mathrm{d}V - k^2\int_K \Pi u\,\overline{w}\,\mathrm{d}V = \int_K \nabla u\cdot\overline{\nabla w}\,\mathrm{d}V - k^2\int_K u\,\overline{w}\,\mathrm{d}V,$$

that implies the assertion. □

**Proposition 4.2.** *If the stabilization form satisfies the following condition: for all $K \in \mathcal{T}_h$ and $v \in V_p(K)$,*

$$s^K((I-\Pi)v,(I-\Pi)v) \geq \|\nabla(I-\Pi)v\|^2_{0,K}\,, \tag{4.1}$$

*then the Gårding inequality for the discrete operator holds true:*

$$\mathrm{Re}[b_h(v,v)] + 2k^2\,\|v\|^2_{0,\Omega} \geq \|v\|^2_{1,k,\mathcal{T}_h} \qquad \forall v \in V_p(\mathcal{T}_h).$$

*Proof.* We will make use of the trivial identity

$$\|v_1+v_2\|^2_{0,K} = \|v_1\|^2_{0,K} + \|v_2\|^2_{0,K} + 2\,\mathrm{Re}\Big[\int_K v_1\overline{v}_2\,\mathrm{d}V\Big]. \tag{4.2}$$

Due to the definition (2.18) of $b_h(\cdot,\cdot)$ and identity (4.2) with $v_1 = \Pi v$ and $v_2 = (I-\Pi)v$, we have

$$\begin{aligned}
\mathrm{Re}[b_h(v,v)] + 2k^2\,\|v\|^2_{0,\Omega} &= a_h(v,v) + 2k^2\,\|v\|^2_{0,\Omega}\\
&= \sum_{K\in\mathcal{T}_h}\Big[a^K(\Pi v,\Pi v) + 2k^2\,\|\Pi v\|^2_{0,K}\Big]\\
&\quad + \sum_{K\in\mathcal{T}_h}\Big[s^K((I-\Pi)v,(I-\Pi)v)) + 2k^2\,\|(I-\Pi)v\|^2_{0,K}\Big]\\
&\quad + \sum_{K\in\mathcal{T}_h} 4k^2\,\mathrm{Re}\Big[\int_K \Pi v\,\overline{(I-\Pi)v}\,\mathrm{d}V\Big]\\
&\geq \sum_{K\in\mathcal{T}_h}\Big[\|\nabla\Pi v\|^2_{0,K} + k^2\,\|\Pi v\|^2_{0,K}\Big] + \sum_{K\in\mathcal{T}_h}\Big[\|\nabla(I-\Pi)v\|^2_{0,\Omega} + 2k^2\,\|(I-\Pi)v\|^2_{0,K}\Big]\\
&\quad + \sum_{K\in\mathcal{T}_h} 2Re\Big[\int_K \nabla\Pi v\cdot\overline{\nabla(I-\Pi)v}\,\mathrm{d}V\Big] + \sum_{K\in\mathcal{T}_h} 2k^2Re\Big[\int_K \Pi v\,\overline{(I-\Pi)v}\,\mathrm{d}V\Big],
\end{aligned}$$

where in the last step we have used (4.1) and Lemma 4.1. By using (4.2) with $v_1 = \nabla\Pi v$, $v_2 = \nabla(I-\Pi)v$, and then with $v_1 = \Pi v$, $v_2 = (I-\Pi)v$, we conclude

$$\mathrm{Re}[b_h(v,v)] + 2k^2\,\|v\|^2_{0,\Omega} \geq \|\nabla v\|^2_{0,\Omega} + k^2\,\|v\|^2_{0,\Omega} = \|v\|^2_{1,k,\mathcal{T}_h}\,.$$ □

Under the assumption of Proposition 4.2, the Gårding's inequality of Theorem 3.1 holds true with $\alpha = 1$.

### 4.1. Choice of $s^K(\cdot,\cdot)$

A first attempt in the choice of the stabilization term could be done by defining

$$s^K((I-\Pi)u,(I-\Pi)v) = \int_K \nabla(I-\Pi)u \cdot \overline{\nabla(I-\Pi)v}\,\mathrm{d}V, \tag{4.3}$$

so that (4.1) is satisfied with the equality.

We notice that the continuity of the discrete bilinear form $a_h(.,.)$ follows from the continuity of the continuous bilinear forms and the continuity of the operator $\Pi$ (see Proposition 2.3). Therefore, (3.1) holds with $\gamma \geq 1 + 2(\beta_{\min}^{-2} + \beta_{\min}^{-1})$, where $\beta_{\min} = \min_{K\in\mathcal{T}_h} \beta(h_K k) = \beta(hk)$.

The matrix form of this stabilization term is

$$(\overline{I-P})^T A(I-P),$$

where where $I$ is the identity matrix of appropriate size (number of directions $p$ times number of mesh vertices $n_K$), $P$ is the matrix representing the operator $\Pi$ defined in Section 2.4 and $A$ is the matrix of entries

$$A(r,s) = \int_K \nabla\psi_s \cdot \overline{\nabla\psi}_r\,\mathrm{d}V.$$

However, when $K$ is a generic polygon, we do not resort to explicit expressions of the basis functions $\varphi_j$ of $V(K)$, and thus of $\psi_r$, but we approximate (4.3).

Adapting the rationale of VEM for elliptic problem to our case, we construct the (approximated) stabilization form as follows. Let $\psi_r(\mathbf{x}) = \varphi_j(\mathbf{x})\,\pi_{j\ell}(\mathbf{x})$ and $\psi_s(\mathbf{x}) = \varphi_\kappa(\mathbf{x})\,\pi_{\kappa m}(\mathbf{x})$ be two basis functions in $V_p(K)$. Then

$$\begin{aligned}\nabla\psi_r &= (\nabla\varphi_j + \varphi_j\, ik\mathbf{d}_\ell)\,\pi_{j\ell},\\ \nabla\psi_s &= (\nabla\varphi_\kappa + \varphi_\kappa\, ik\mathbf{d}_m)\,\pi_{\kappa m},\end{aligned}$$

and thus

$$\nabla\psi_s \cdot \overline{\nabla\psi}_r = (\nabla\varphi_\kappa\cdot\nabla\varphi_j + ik\,\varphi_\kappa\,\mathbf{d}_m\cdot\nabla\varphi_j - ik\,\varphi_j\,\mathbf{d}_\ell\cdot\nabla\varphi_\kappa + k^2\varphi_\kappa\,\varphi_j\,\mathbf{d}_m\cdot\mathbf{d}_\ell)\,\pi_{\kappa m}\,\overline{\pi}_{j\ell}.$$

Taking into account the scaling of the terms in the brackets with respect to the elemental mesh size, we neglect the last three and replace the first by $\delta_{\kappa j}/h_K^2$. Therefore, we define $s^K((I-\Pi)u,(I-\Pi)v)$ in terms of its associated matrix $S_K$ as

$$S_K = \overline{(I-P)}^T M(I-P), \tag{4.4}$$

where $M$ is the (scaled) plane wave mass matrix of size $(n_K p, n_K p)$ whose entries are $M(r,s) = \int_K \frac{\delta_{\kappa j}}{h_K^2}\,\pi_{\kappa m}\,\overline{\pi}_{j\ell}\,\mathrm{d}V$. More precisely, if $r = (j-1)p+\ell$ and $s = (\kappa-1)p+m$,

$$\begin{aligned}M(r,s) &= \frac{\delta_{\kappa j}}{h_K^2}\,\mathrm{e}^{ik\mathbf{d}_m\cdot(\mathbf{x}_K-\mathbf{x}_j)}\,\mathrm{e}^{-ik\mathbf{d}_\ell\cdot(\mathbf{x}_K-\mathbf{x}_\kappa)}\int_K \pi_m\,\overline{\pi}_\ell\,\mathrm{d}V\\ &= \frac{\delta_{\kappa j}}{h_K^2}\,\mathrm{e}^{ik\mathbf{d}_m\cdot(\mathbf{x}_K-\mathbf{x}_j)}\,\mathrm{e}^{-ik\mathbf{d}_\ell\cdot(\mathbf{x}_K-\mathbf{x}_\kappa)}\int_K \mathrm{e}^{ik(\mathbf{d}_m-\mathbf{d}_\ell)\cdot(\mathbf{x}-\mathbf{x}_K)}\mathrm{d}V.\end{aligned} \tag{4.5}$$

We point out that the integral defining $M(r,s)$ can be computed exactly (see Rem. 2.5).

On each element $K$, the elemental matrix of the complete PW-VEM is therefore

$$\overline{B}^T\overline{G}^{-1}B + \overline{(I-P)}^T M(I-P) + R \tag{4.6}$$

where $D$, $B$, $G$ and $P$ are defined in Section 2.4, $M$ is the scaled plane wave mass matrix defined in (4.5), and $R$ is the matrix associated with the bilinear form $ik\int_{\partial K\cap\partial\Omega} u\overline{v}\,dS$:

$$R(r,s) = ik\int_{\partial K\cap\partial\Omega} \psi_s\overline{\psi}_r\,\mathrm{d}S, \qquad r,s = 1,\ldots,n_K p.$$

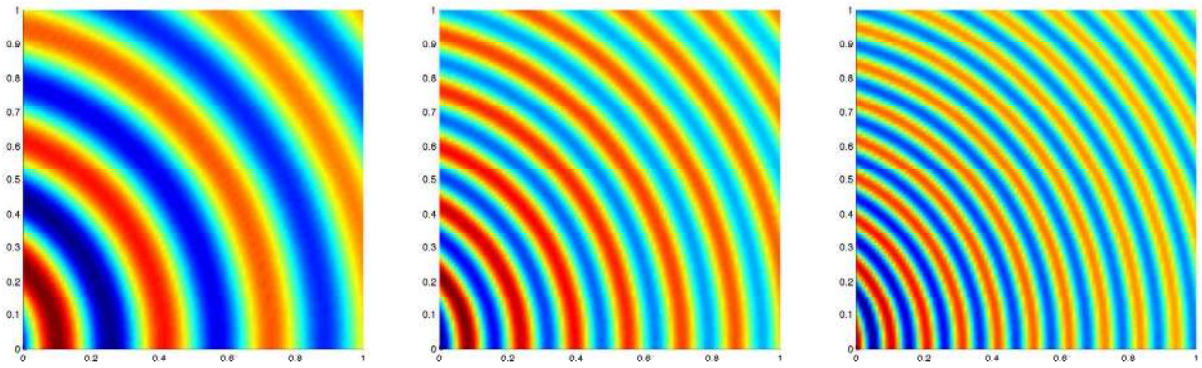

FIGURE 1. Real part of the function $u(\mathbf{x}) = H_0^{(1)}(k\,|\mathbf{x}-\mathbf{x}_0|)$, $\mathbf{x}_0 = (-0.25, 0)$ in the domain $\Omega = (0,1)^2$, for $k = 20$ (*left*), $k = 40$ (*center*), and $k = 60$ (*right*).

## 5. Numerical results

Unless otherwise stated, in the following experiments we consider the problem (2.1) in the domain $\Omega = (0,1)^2$, and with boundary datum $g$ such that the analytical solution is

$$u(\mathbf{x}) = H_0^{(1)}(k\,|\mathbf{x}-\mathbf{x}_0|), \qquad \mathbf{x}_0 = (-0.25, 0),$$

where $H_0^{(1)}$ is the zero-th order Hankel function of the first kind. In Figure 1, we report the real part of this solution $u$ for the wave numbers $k = 20$, $k = 40$ and $k = 60$. All the errors reported in the following are relative errors in the $L^2$-norm.

The function $u(\mathbf{x})$ is a regular solution of the homogeneous Helmholtz problem, so that the $h$-convergence result of Corollary 3.4 provides order $h^m$ (with $m = (p-1)/2$) for the error in the $\|.\|_{1,k,\mathcal{T}_h}$ norm. An $L^2$-error bound is then given by (3.12). Because of the restriction (3.13) on the mesh size, we have $hk^2 < C$ and the factor $hk$ in (3.12) implies the gain of a factor $h^{1/2}$ for the $L^2$-error, with respect to the $\|.\|_{1,k,\mathcal{T}_h}$-error.

Due to the fact that high-order approximation properties of the plane wave spaces hold true only for solutions to the homogeneous Helmholtz equation, and our duality argument in the proof of Theorem 3.1 makes use of a dual problem with non zero right-hand side (see Eq. (3.8)), our analysis does not cover the asymptotics in $p$. On the other hand, the $p$-version of the best approximation results ([30], Thm. 3.9 and Rem. 3.13, and [33], Sect. 5.2, for the best approximation estimates in $V_p^*(\mathcal{T}_h)$; for $V_p(\mathcal{T}_h)$, use again [39], Thm. 2.1) give algebraic convergence $(\log(p)/p)^\ell$, provided that the exact solution belongs to $H^{\ell+1}(\Omega)$ and $p$ is large enough, or exponential convergence, whenever the exact solution can be extended analytically outside $\Omega$. Therefore, we also present numerical results for fixed $h$ and increasing $p$.

First, we numerically evaluate in Section 5.1 the loss of accuracy due to the approximation of the stabilization term. Then, in Section 5.2, we test the $h$- and $p$-versions of the PW-VEM on polygonal meshes, and compare the results obtained for different values of the wave number $k$. We conclude by testing the $p$-convergence for non analytic exact solutions (Sect. 5.2.3).

### 5.1. Effects of the approximation of the stabilization term

We recall that the choice $s^K((I-\Pi)u,(I-\Pi)v) = a^K((I-\Pi)u,(I-\Pi)v)$ in the formulation (2.18) coincides with the partition of unity (PUM) method, since the complete bilinear form is considered in this case. On triangular meshes, where the canonical VEM basis functions $\varphi_j$ coincide with the classical Lagrangian $\mathbb{P}_1$ basis functions, we compare the error of the PUM, with that of the VEM with the stabilization (4.3) (GRAD in the following) and that of the PW-VEM, whose elemental matrices are given by (4.6).

TABLE 1. Relative error in the $L^2$-norm for PUM, GRAD, PW-VEM for structured triangular meshes; $k = 20$, $p = 13$.

| | PUM | | GRAD | | PW-VEM | |
|---|---|---|---|---|---|---|
| $h$ | $L^2$-error | rate | $L^2$-error | rate | $L^2$-error | rate |
| 7.0711e−01 | 1.9213e−02 | – | 7.1989e−01 | – | 4.1548e−01 | – |
| 3.5355e−01 | 4.0683e−04 | 5.5615 | 1.5517e−03 | 8.8577 | 1.0990e−02 | 5.2406 |
| 1.7678e−01 | 3.4126e−06 | 6.8974 | 3.3981e−06 | 8.8349 | 1.2969e−04 | 6.4050 |
| 8.8388e−02 | 4.0164e−08 | 6.4088 | 4.0148e−08 | 6.4033 | 1.1089e−06 | 6.8698 |

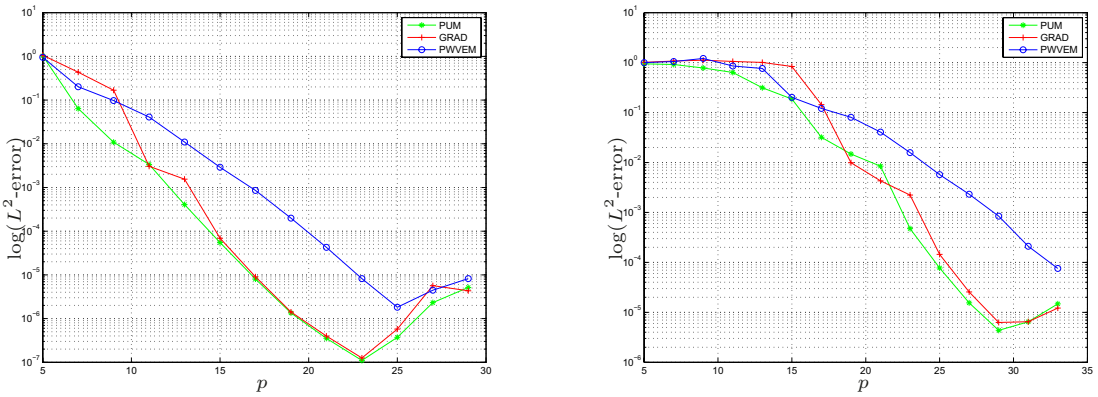


FIGURE 2. Relative error in the $L^2$-norm for PUM, GRAD, PW-VEM for the structured triangular mesh with 32 elements ($h$ =3.5355e−01), for different values of $p$, for $k = 20$ (*left*) and $k = 40$ (*right*).

We have used structured triangular meshes, obtained from Cartesian subdivisions of $\Omega$, dividing then each square into two triangles by one of the diagonals. We report in Table 1 the results obtained on four meshes containing, respectively, 8, 32, 128 and 512 triangles, using $p = 13$ plane waves per node, for the wave number $k = 20$. When the mesh size $h$ is sufficiently small, GRAD is very close to PUM, showing that the sufficient requirement (4.1) on the stabilization term is indeed sharp. When the approximation of the stabilization term defined in (4.4)–(4.5) is used instead (PW-VEM), some accuracy is lost. However, the same order of convergence as for PUM is maintained.

We also report in Figure 2 the errors with the three methods on the mesh with 32 elements, varying $p$, for $k = 20$ and $k = 40$, respectively. As in the $h$-error study, when the best approximation error is sufficiently small (here, the number of plane waves per node is sufficiently large), GRAD coincides with PUM, and PW-VEM looses some accuracy, but still showing an exponential convergence behavior, with a comparable order of convergence. Notice that, when increasing the wave number $k$, all these methods exhibit a larger preasymptotic region with slower convergence. Moreover, in both figures, and in many of the next plots, for large values of $p$, instability takes place due to the ill-conditioning of the plane wave basis, and the impact of roundoff error results in the increasing of the error; we refer to [30] for a similar behavior of the plane wave discontinuous Galerkin (PWDG) method. We remark that a similar phenomenon occurs for small $h$ (see Sect. 5.2 below).

We point out that the tests presented above do not provide a complete comparison between the PW-VEM and PUM (and/or GRAD), since we restricted to triangular meshes, where PUM can be exactly computed. A fair comparison should be carried out on more general meshes, where the use of PUM would need some quadrature formulas (we refer to [37], where a PUM with generalized barycentric coordinates is compared to VEM with different stabilizations for the Poisson's problem). On the other hand, these tests on triangular meshes suggest that there is a margin of improvement for the choice of the approximation of the stabilization term defined in (4.4) and (4.5).

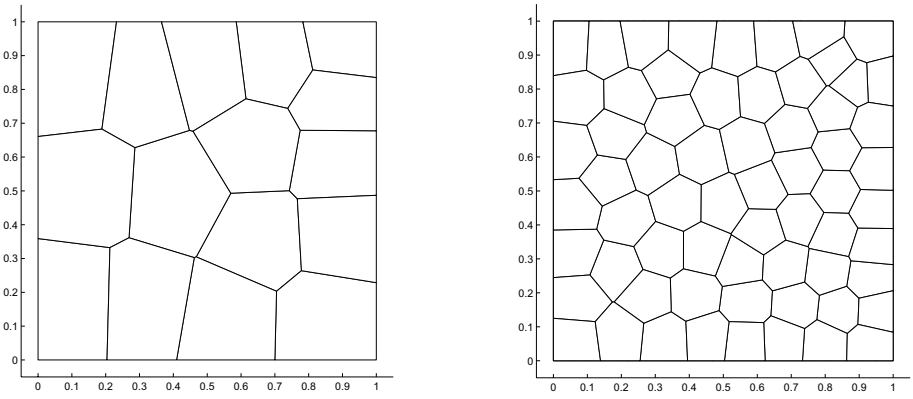

FIGURE 3. Voronoi's meshes with 16 (*left*) and 64 (*right*) elements.

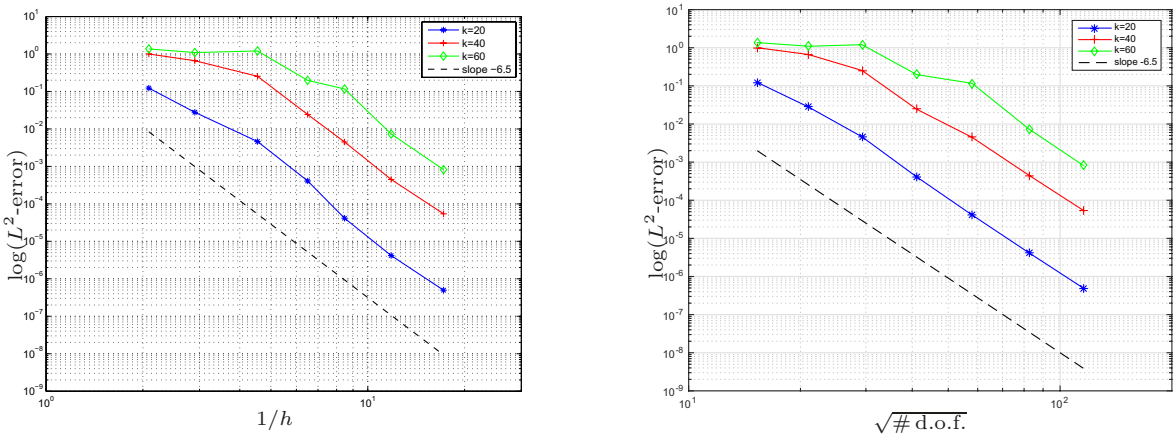


FIGURE 4. Relative error in the $L^2$-norm of the PW-VEM for $p = 13$ and $k = 20, 40, 60$ on the Voronoi's meshes.

## 5.2. Convergence

We test convergence of the PW-VEM on (polygonal) Voronoi's meshes made of $2^n$ elements, $3 \leq n \leq 9$. We report in Figure 3 the meshes with 16 and 64 elements.

### *5.2.1. h-convergence*

We test first the $h$-convergence. We report in Figure 4 the relative errors in the $L^2$-norm of the PW-VEM method on the Voronoi's meshes, for $p = 13$ and $k = 20, 40, 60$. As pointed out at the beginning of Section 5, the expected convergence rate in $h$ is $m + 1/2$, *i.e.*, 6.5 for $p = 13$. This rate seems to be actually reached, after a pre-asymptotic region, which is wider for larger $k$. Also the results of Table 2 seem to confirm these rates (6.5 for $p = 13$ and 7.5 for $p = 15$). In both Figure 4 and Table 2, the convergence rates are measured considering the error as a function of $h$, as well as of the square root of the number of degrees of freedom of $V_p(\mathcal{T}_h)$ (equal to $p$ times the number of the mesh vertices). However, since the sequence of Voronoi's meshes considered here is not made by nested meshes, the maximum of the diameters of the elements $K \in \mathcal{T}_h$ (definition of $h$ for Tab. 2), as well as the number of the mesh vertices, does not vary by a factor from one mesh to the other, so that a precise assessment of the convergence rate is difficult. Nevertheless, we can conclude that high order rate is

TABLE 2. Relative error in the $L^2$-norm and convergence rates for PW-VEM for $k = 20$, with $p = 13$ and $p = 15$, on Voronoi's meshes.

| | $p = 13$ | | | | $p = 15$ | | | |
|---|---|---|---|---|---|---|---|---|
| $h$ | $d.o.f.$ | $L^2$-error | $h$-rate | $\sqrt{d.o.f.}$-rate | $d.o.f.$ | $L^2$-error | $h$-rate | $\sqrt{d.o.f.}$-rate |
| 3.4487e−01 | 442 | 2.7882e−02 | – | – | 510 | 1.1374e−02 | – | – |
| 2.2017e−01 | 858 | 4.6014e−03 | 4.0147 | 5.4323 | 990 | 1.5253e−03 | 4.4772 | 6.0581 |
| 1.5376e−01 | 1690 | 4.0962e−04 | 6.7374 | 7.1366 | 1950 | 6.6821e−05 | 8.7123 | 9.2286 |
| 1.1806e−01 | 3354 | 4.1264e−05 | 8.6874 | 6.6973 | 3870 | 5.3076e−06 | 9.5868 | 7.3907 |
| 8.4571e−02 | 6682 | 4.1597e−06 | 6.8785 | 6.6580 | 7710 | 9.3361e−07 | 5.2096 | 5.0426 |

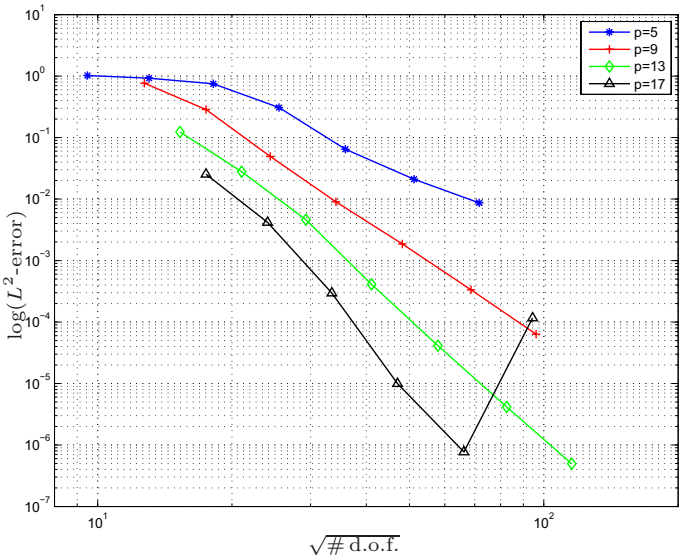


FIGURE 5. Relative error in the $L^2$-norm of the PW-VEM for $k = 20$ and different values of $p$ on the Voronoi's meshes.

provided also on polygonal meshes. We also report in Figure 5 the error plots for $k = 20$ and for different values of $p$. For fine meshes and high $p$, instability takes place and the error increases, as already observed.

In order to test the pollution effect, we have run the PW-VEM, with $p = 9$, on the Voronoi's meshes made of $2^n$ elements, $3 \leq n \leq 9$, and $k$ chosen such that the product $hk$ is the constant 3 (*i.e.*, $k = 6.26$, 8.70, 13.63, 19.51, 25.41, 35.47, 51.59, respectively). The results reported in Figure 6 confirm that the $h$-version of the PW-VEM is affected by pollution, *i.e.*, the boundedness of the product $hk$ is not sufficient to guarantee convergence of the discretization error.

*5.2.2. p-convergence*

In Figure 7, we report the relative errors in the $L^2$-norm for different values of $p$ in the case $k = 20$, on the Voronoi's meshes with 16 and 64 elements (34 and 130 vertices, respectively). For the first mesh, $p$ varies from 5 to 31, for the second mesh from 5 to 23. We see exponential convergence in the number of degrees of freedom, before the onset of instability for high $p$, as in Figure 2, *left*, for the triangular meshes. In the case of larger elements (Fig. 7, *left*), the pre-asymptotic region is wider, while for smaller elements (Fig. 7, *right*), the onset of instability occurs for smaller values of $p$. Notice that the considered meshes also contain edges which are small, as compared to the mesh size. These results, together with those in Section 5.2.1, thus suggest that the PW-VEM is robust in case of degenerating sides.

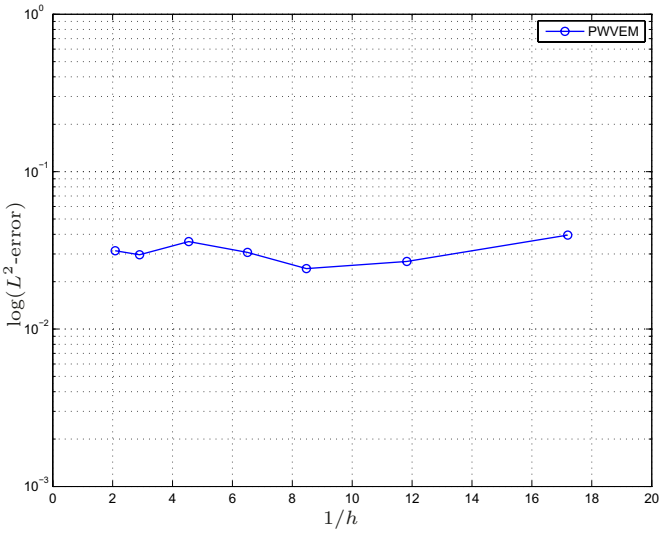


FIGURE 6. Relative error in the $L^2$-norm of the PW-VEM on the Voronoi's meshes for $hk = 3$ and for $p = 9$.

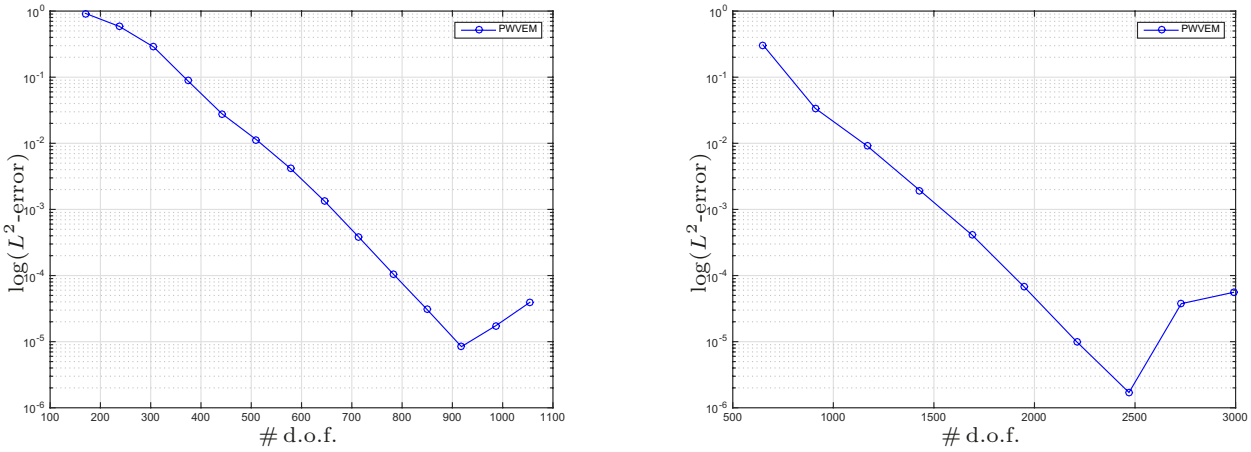


FIGURE 7. Relative error in the $L^2$-norm for PW-VEM for $k = 20$ on Voronoi's meshes with 16 (*left*) and 64 (*right*) elements, for different values of $p$.

In Figure 8, a polygonal mesh with non convex elements (100 elements, 202 vertices) is represented, and the corresponding $L^2$-error for $k = 20$ and different values of $p$ (ranging from 5 to 21) is plotted. The results are comparable to those obtained with meshes with convex elements. Due to the presence of small elements, onset of instability occurs for smaller values of $p$, as compared to the previous, more regular, meshes.

We compare now the convergence behaviour of the PW-VEM for different values of the wavenumber $k$. We plot in Figure 9 the $L^2$-error of the PW-VEM on the Voronoi's mesh with 64 elements and 130 vertices, for different values of $p$ and for $k = 20$, 40, 60; for $k = 20$, $p$ varies from 5 to 23, for $k = 40$ from 5 to 31, and for $k = 60$ from 5 to 35. For larger values of $k$, the pre-asymptotic region is wider, while onset of instability occurs for larger values of $p$.

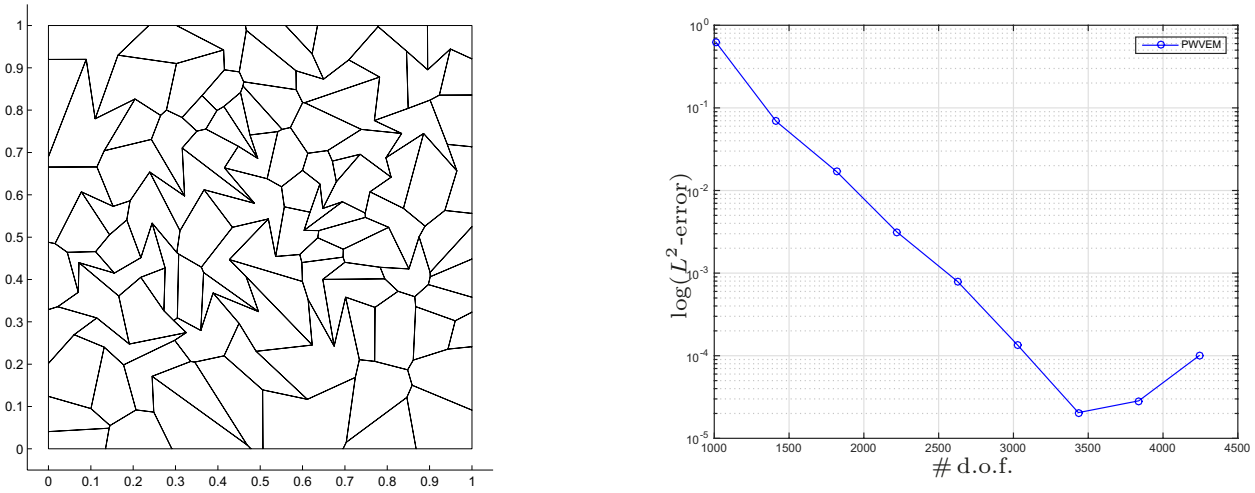


FIGURE 8. Polygonal mesh with 100 elements and 202 vertices containing non convex elements (*left*), and relative error in the $L^2$-norm for PW-VEM for $k = 20$ and different values of $p$ (*right*).

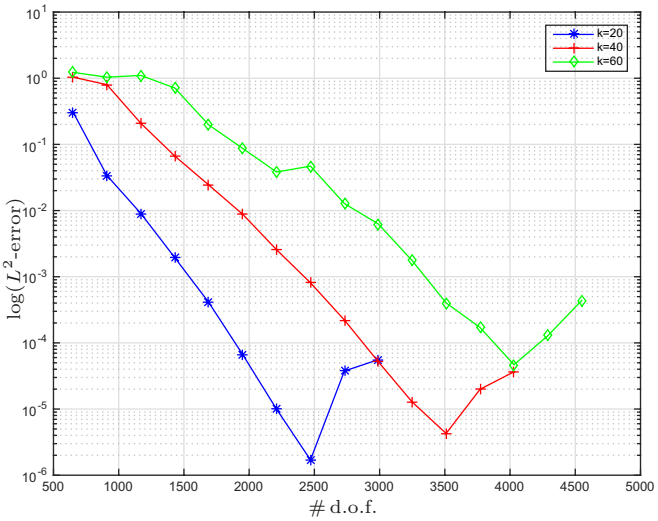


FIGURE 9. Relative error in the $L^2$-norm of the PW-VEM on the Voronoi's mesh with 64 elements, for different values of $p$ and for $k = 20, 40, 60$.

*5.2.3. p-convergence for non smooth solutions*

Finally, we test the $p$-convergence in the case of solutions with low regularity. To this aim, as in Section 4 of [30], we consider now the problem (2.1) again in the domain $\Omega = (0,1)^2$, and with boundary datum $g$ such that the analytical solution is given, in polar coordinates $\mathbf{x} = (r\cos\vartheta, r\sin\vartheta)$, by

$$u(\mathbf{x} - \mathbf{x}_0) = J_\xi(kr)\cos(\xi\vartheta), \qquad \xi \geq 0,\ \mathbf{x}_0 = (0, 0.5), \tag{5.1}$$

where $J_\xi$ is the Bessel function of the first kind and order $\xi$. We choose $k = 10$. For integer $\xi$, $u$ can be extended analytically outside $\Omega$, otherwise its derivatives have a singularity at $\mathbf{x}_0$. We report in Figure 10 the real part of $u$ for $\xi = 1$ (regular case), $\xi = 3/2$ ($u \in H^2(\Omega)$) and $\xi = 2/3$ ($u \notin H^2(\Omega)$).

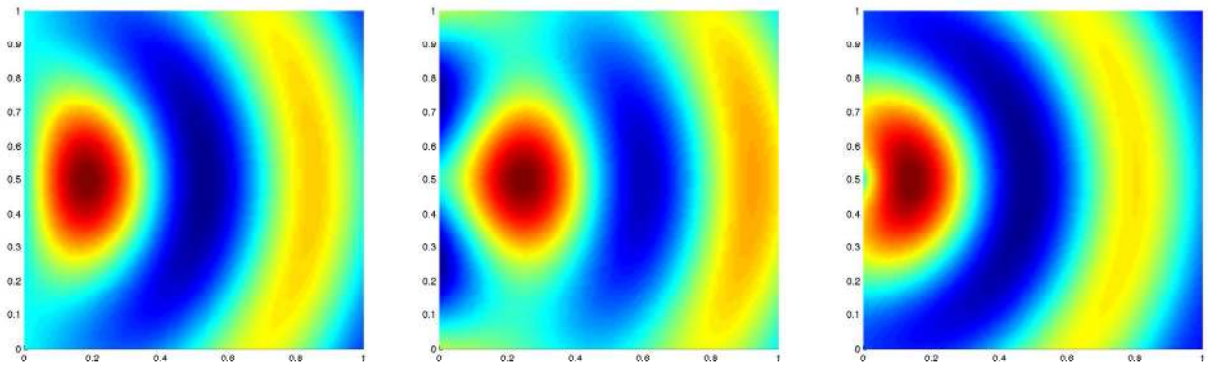

FIGURE 10. Real part of the function $u(\mathbf{x}-\mathbf{x}_0) = J_\xi(kr)\cos(\xi\vartheta)$, $\mathbf{x}_0 = (0, 0.5)$ in the domain $\Omega = (0,1)^2$, for $k = 10$ and $\xi = 1$ (*left*), $\xi = 3/2$ (*center*), and $\xi = 2/3$ (*right*).

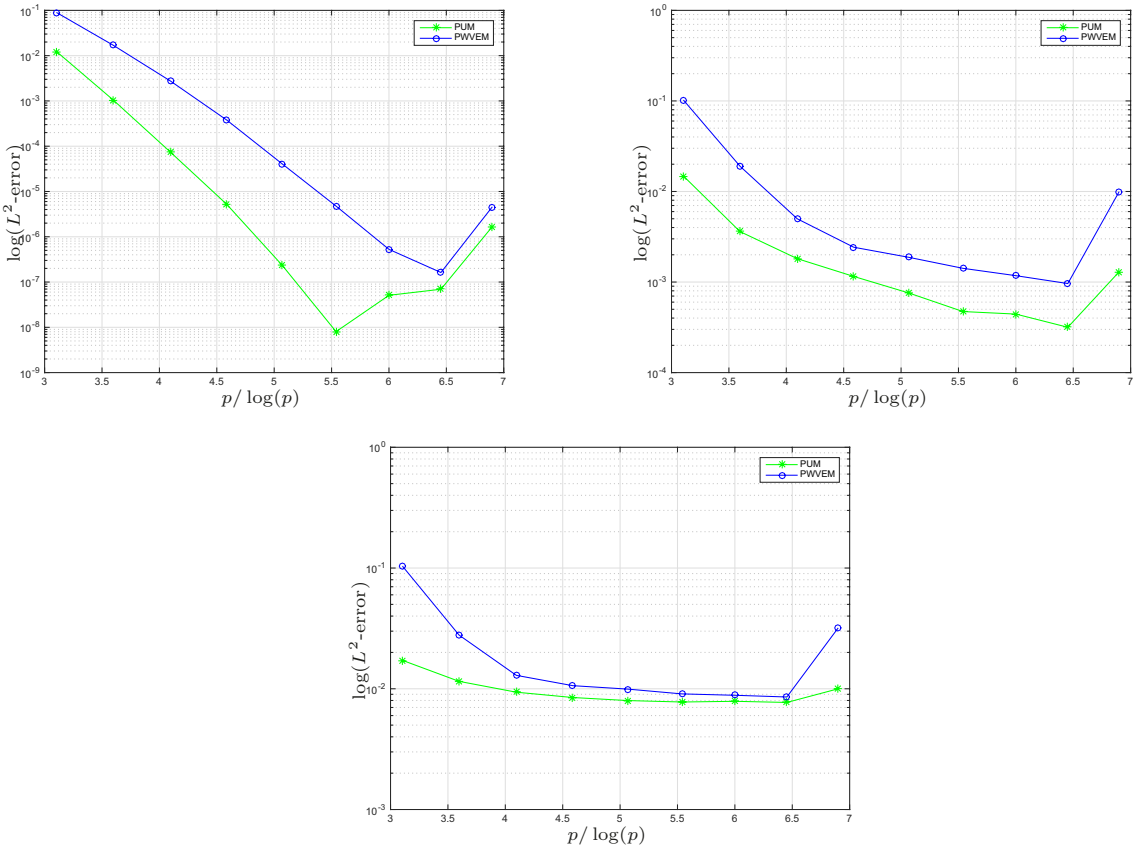


FIGURE 11. Relative error in the $L^2$-norm of the PW-VEM and PUM on the structured triangular mesh with 32 elements, for the model problem with exact solution (5.1) for $k = 10$ and $\xi = 1$ (*top, left*), $\xi = 3/2$ (*top, right*), and $\xi = 2/3$ (*bottom*), for different values of $p$.

We report in Figure 11 the relative errors in the $L^2$-norm for the three cases, obtained on the structured triangular mesh with 32 elements, for different values of $p$. While for the smooth solution ($\xi = 1$) we have

exponential convergence, before the onset of instability, as in the previous experiments, in the other two cases the convergence is algebraic, even if the rates are unclear, the results for $\xi = 3/2$ being better than those for $\xi = 2/3$. Similar results were obtained in [30] for the PWDG method. We also report the results obtained with the PUM, for the sake of comparison (this is the reason why we have used triangular meshes).

## 6. Conclusions

We have presented a first PW-VEM scheme for the discretization of the Helmholtz equation. $H^1$-conformity is guaranteed by the VEM framework, while high order convergence for the homogeneous problem, for smooth analytical solutions, is achieved through a plane wave enrichment of the approximating spaces. An $h$-version error analysis of the PW-VEM is derived, while numerical results also show exponential convergence of the $p$-version for smooth analytical solutions. These preliminary results highlight that a suitable interplay of $h$, $p$ and $k$ is important in order to obtain quasi-optimality, and suggest that similar results as those of the complete $hp$-analysis of [41] could hold.

Several restrictions on the model problem we have considered could be easily removed, and the method could be extended from 2D to 3D, and to acoustic scattering problems. The extension of the method and its analysis to problems with non constant coefficients or non zero source terms is also an interesting issue. Exploring alternative choices for the stabilization term, the projection operator $\Pi$ and/or of the space onto which to project, as well as extensions to non uniform $p$ and higher order VEM will be subject of future research.

*Acknowledgements.* The authors are grateful to L. Beirão da Veiga, F. Brezzi and L.D. Marini for stimulating and fruitful discussions. Ilaria Perugia and Paola Pietra acknowledge support of the Italian Ministry of Education, University and Research (MIUR) through the project PRIN-2012HBLYE4.

## References

[1] P.F. Antonietti, L. Beirão da Veiga, D. Mora and M. Verani, A stream virtual element formulation of the Stokes problem on polygonal meshes. *SIAM J. Numer. Anal.* **52** (2014) 386–404.

[2] B. Ayuso de Dios, K. Lipnikov and G. Manzini, The nonconforming virtual element method. To appear in Special issue – Polyhedral discretization for PDE. *ESAIM: M2AN* **50** (2016). DOI:10.1051/m2an/2015090

[3] I.M. Babuška and S.A. Sauter, Is the pollution effect of the FEM avoidable for the Helmholtz equation? *SIAM Rev.* **42** (2000) 451–484.

[4] L. Beirão da Veiga and G. Manzini, A virtual element method with arbitrary regularity. *IMA J. Numer. Anal.* **34** (2014) 759–781.

[5] L. Beirão da Veiga, F. Brezzi, A. Cangiani, G. Manzini, L.D. Marini and A. Russo, Basic principles of virtual element methods. *Math. Models Methods Appl. Sci.* **23** (2013) 199–214.

[6] L. Beirão da Veiga, F. Brezzi and L.D. Marini, Virtual elements for linear elasticity problems. *SIAM J. Numer. Anal.* **51** (2013) 794–812.

[7] L. Beirão da Veiga, F. Brezzi, L.D. Marini and A. Russo, $H(\mathrm{div})$ and $H(\mathrm{curl})$-conforming virtual element method. To appear in *Numer. Math.* (2015). DOI:10.1007/s00211-015-0746-1

[8] L. Beirão da Veiga, F. Brezzi, L.D. Marini and A. Russo, Mixed virtual element methods for general second order elliptic problems. To appear in Special issue – Polyhedral discretization for PDE. *ESAIM M2AN* **50** (2016). DOI:10.1051/m2an/2015067

[9] L. Beirão da Veiga, F. Brezzi, L.D. Marini and A. Russo, Virtual element methods for general second order elliptic problems on polygonal meshes. *Math. Models Methods Appl. Sci.* **26** (2016) 729–750.

[10] L. Beirão Da Veiga, F. Brezzi, L.D. Marini and A. Russo, The Hitchhiker's guide to the virtual element method. *Math. Models Methods Appl. Sci.* **24** (2014) 1541–1573.

[11] L. Beirão da Veiga, C. Lovadina and D. Mora, A virtual element method for elastic and inelastic problems on polytope meshes. *Comput. Methods Appl. Mech. Eng.* **295** (2015) 327–346.

[12] M.F. Benedetto, S. Berrone, S. Pieraccini and S. Scialò, The virtual element method for discrete fracture network simulations. *Comput. Methods Appl. Mech. Eng.* **280** (2014) 135–156.

[13] J.H. Bramble and L.E. Payne, Bounds in the Neumann problem for second order uniformly elliptic operators. *Pacific J. Math* **12** (1962) 823–833.

[14] F. Brezzi and L.D. Marini, Virtual element methods for plate bending problems. *Comput. Methods Appl. Mech. Eng.* **253** (2013) 455–462.

[15] F. Brezzi and L.D. Marini, Virtual Element and Discontinuous Galerkin Methods. In Recent Developments in Discontinuous Galerkin Finite Element Methods for Partial Differential Equations. Springer (2014) 209–221.

[16] F. Brezzi, R.S. Falk and L.D. Marini, Basic principles of mixed virtual element methods. *ESAIM: M2AN* **48** (2014) 1227–1240.
[17] A. Buffa and P. Monk, Error estimates for the Ultra Weak Variational Formulation of the Helmholtz equation. *ESAIM: M2AN* **42** (2008) 925–940.
[18] O. Cessenat, *Application d'une nouvelle formulation variationnelle aux équations d'ondes harmoniques, Problèmes de Helmholtz 2D et de Maxwell 3D*. Ph.D. thesis, Université Paris IX Dauphine (1996).
[19] O. Cessenat and B. Després, Application of an ultra weak variational formulation of elliptic PDEs to the two-dimensional Helmholtz equation. *SIAM J. Numer. Anal.* **35** (1998) 255–299.
[20] E. Deckers, O. Atak, L. Coox, R. D'Amico, H. Devriendt, S. Jonckheere, K. Koo, B. Pluymers, D. Vandepitte and W. Desmet, The wave based method: An overview of 15 years of research. Innovations in Wave Modelling. *Wave Motion* **51** (2014) 550–565.
[21] W. Desmet, *A wave based prediction technique for coupled vibro-acoustic analysis*. Ph.D. thesis, KU Leuven, Belgium, 1998.
[22] C. Farhat, I. Harari and L. Franca, The discontinuous enrichment method. *Comput. Methods Appl. Mech. Eng.* **190** (2001) 6455–6479.
[23] C. Farhat, I. Harari and U. Hetmaniuk, A discontinuous Galerkin method with Lagrange multipliers for the solution of Helmholtz problems in the mid-frequency regime. *Comput. Methods Appl. Mech. Eng.* **192** (2003) 1389–1419.
[24] G. Gabard, Discontinuous Galerkin methods with plane waves for time-harmonic problems. *J. Comput. Phys.* **225** (2007) 1961–1984.
[25] G. Gabard, Exact integration of polynomial-exponential products with application to wave-based numerical methods. *Comm. Numer. Methods Eng.* **25** (2009) 237–246.
[26] A.L. Gain, C. Talischi and G.H. Paulino, On the virtual element method for three-dimensional linear elasticity problems on arbitrary polyhedral meshes. *Comput. Methods Appl. Mech. Eng.* **282** (2014) 132–160.
[27] C.J. Gittelson, *Plane wave discontinuous Galerkin methods*. Master's thesis, SAM-ETH Zürich, Switzerland (2008).
[28] C.J. Gittelson, R. Hiptmair and I. Perugia, Plane wave discontinuous Galerkin methods: analysis of the *h*-version. *ESAIM: M2AN* **43** (2009) 297–332.
[29] R. Hiptmair, A. Moiola and I. Perugia, *Approximation by plane waves*. Technical report 2009-27, SAM-ETH Zürich, Switzerland (2009). Available at http://www.sam.math.ethz.ch/reports/2009/27.
[30] R. Hiptmair, A. Moiola and I. Perugia, Plane wave discontinuous Galerkin methods for the 2D Helmholtz equation: analysis of the *p*-version. *SIAM J. Numer. Anal.* **49** (2011) 264–284.
[31] R. Hiptmair, A. Moiola and I. Perugia, Trefftz discontinuous Galerkin methods for acoustic scattering on locally refined meshes. *Appl. Numer. Math.* **79** (2014) 79–91.
[32] R. Hiptmair, A. Moiola and I. Perugia, A Survey of Trefftz Methods for the Helmholtz Equation. "Building Bridges: Connections and Challenges in Modern Approaches to Numerical Partial Differential Equations". Edited by G.R. Barrenechea, A. Cangiani, E.H. Geogoulis. In *Lect. Notes Comput. Sci. Eng.* Springer. Preprint arXiv:1505.04521 [math.NA] (2015).
[33] R. Hiptmair, A. Moiola and I. Perugia, Plane wave discontinuous Galerkin Methods: Exponential convergence of the *hp*-version. To appear in *Found. Comput. Math.* (2015). DOI:10.1007/s10208-015-9260-1
[34] F. Ihlenburg and I. Babuska, Solution of Helmholtz problems by knowledge-based fem. *Comp. Ass. Mech. Eng. Sci.* **4** (1997) 397–416.
[35] J. Ladevèze and P. Ladevèze, Bounds of the Poincaré constant with respect to the problem of star-shaped membrane regions. *Z. Angew. Math. Phys.* **29** (1978) 670–683.
[36] P. Ladevèze and H. Riou, On Trefftz and weak Trefftz discontinuous Galerkin approaches for medium-frequency acoustics. *Comput. Methods Appl. Mech. Eng.* **278** (2014) 729–743.
[37] G. Manzini, A. Russo and N. Sukumar. New perspectives on polygonal and polyhedral finite element methods. *Math. Models Methods Appl. Sci.* **24** (2014) 1665–1699.
[38] J.M. Melenk, *On Generalized Finite Element Methods*. Ph.D. thesis, University of Maryland, 1995.
[39] J.M. Melenk and I. Babuška, The partition of unity finite element method: basic theory and applications. *Comput. Methods Appl. Mech. Eng.* **139** (1996) 289–314.
[40] J.M. Melenk and I Babuska, Approximation with harmonic and generalized harmonic polynomials in the partition of unity method. *Comp. Ass. Mech. Eng. Sci.* **4** (1997) 607–632.
[41] J.M. Melenk and S. Sauter, Wavenumber explicit convergence analysis for Galerkin discretizations of the Helmholtz equation. *SIAM J. Numer. Anal.* **49** (2011) 1210–1243.
[42] A. Moiola, *Trefftz-discontinuous Galerkin methods for time-harmonic wave problems*. Ph.D. thesis, Seminar for applied mathematics, ETH Zürich (2011). Available at http://e-collection.library.ethz.ch/view/eth:4515.
[43] A. Moiola, R. Hiptmair and I. Perugia, Plane wave approximation of homogeneous Helmholtz solutions. *Z. Angew. Math. Phys.* **62** (2011) 809–837.
[44] P. Monk and D.Q. Wang, A least squares method for the Helmholtz equation. *Comput. Methods Appl. Mech. Eng.* **175** (1999) 121–136.
[45] L.E. Payne and H.F. Weinberger, An optimal Poincaré inequality for convex domains. *Arch. Rational Mech. Anal.* **5** (1960) 286–292.
[46] H. Riou, P. Ladevéze and B. Sourcis, The multiscale VTCR approach applied to acoustics problems. *J. Comput. Acoust.* **16** (2008) 487–505.
[47] M. Stojek, Least-squares Trefftz-type elements for the Helmholtz equation. *Int. J. Numer. Methods Eng.* **41** (1998) 831–849.
[48] N. Sukumar and A. Tabarraei, Conforming polygonal finite elements. *Int. J. Numer. Methods Eng.* **61** (2004) 2045–2066.
[49] R. Tezaur and C. Farhat, Three-dimensional discontinuous Galerkin elements with plane waves and Lagrange multipliers for the solution of mid-frequency Helmholtz problems. *Int. J. Numer. Methods Eng.* **66** (2006) 796–815.